

---

# SKADA-Bench: Benchmarking Unsupervised Domain Adaptation Methods with Realistic Validation On Diverse Modalities

**Yanis Lalou\***

*École Polytechnique, IP Paris, CMAP, UMR 7641, 91120 Palaiseau, France*

*yanis.lalou@polytechnique.edu*

**Théo Gnassounou\***

*Université Paris-Saclay, Inria, CEA, 91120 Palaiseau, France*

*theo.gnassounou@inria.fr*

**Antoine Collas\***

*Université Paris-Saclay, Inria, CEA, 91120 Palaiseau, France*

*antoine.collas@inria.fr*

**Antoine de Mathelin\***

*Centre Borelli, ENS Paris-Saclay, Gif-sur-Yvette, 91190, France*

*antoine.demat@gmail.com*

**Oleksii Kachaiev**

*Dipartimento di Matematica, Università degli Studi di Genova, Genoa, Italy*

*oleksii.kachaiev@gmail.com*

**Ambroise Odonnat**

*Noah's Ark Lab, Inria, Paris, France*

*ambroise.odonnat@gmail.com*

**Thomas Moreau**

*Université Paris-Saclay, Inria, CEA, 91120 Palaiseau, France*

*thomas.moreau@inria.fr*

**Alexandre Gramfort**

*Université Paris-Saclay, Inria, CEA, 91120 Palaiseau, France*

*alexandre.gramfort@inria.fr*

**Rémi Flamary**

*École Polytechnique, IP Paris, CMAP, UMR 7641, 91120 Palaiseau, France*

*remi.flamary@polytechnique.edu*

---

\*Equal contribution

---

## Abstract

Unsupervised Domain Adaptation (DA) consists of adapting a model trained on a labeled source domain to perform well on an unlabeled target domain with some data distribution shift. While many methods have been proposed in the literature, fair and realistic evaluation remains an open question, particularly due to methodological difficulties in selecting hyperparameters in the unsupervised setting. With **SKADA-Bench**, we propose a framework to evaluate DA methods on diverse modalities, beyond computer vision tasks that have been largely explored in the literature. We present a complete and fair evaluation of existing shallow algorithms, including reweighting, mapping, and subspace alignment. Realistic hyperparameter selection is performed with nested cross-validation and various unsupervised model selection scores, on both simulated datasets with controlled shifts and real-world datasets across diverse modalities, such as images, text, biomedical, and tabular data. Our benchmark highlights the importance of realistic validation and provides practical guidance for real-life applications, with key insights into the choice and impact of model selection approaches. **SKADA-Bench** is open-source, reproducible, and can be easily extended with novel DA methods, datasets, and model selection criteria without requiring re-evaluating competitors. **SKADA-Bench** is available on Github at <https://github.com/scikit-adaptation/skada-bench>.

## 1 Introduction

Given some training –or *source*– data, supervised learning consists in estimating a function that makes good predictions on *target* data. However, performance often drops when the source distribution used for training differs from the target distribution used for testing. This shift can be due, for instance, to the collection process or non-stationarity in the data, and is ubiquitous in real-life settings. It has been observed in various application fields, including tabular data (Gardner et al., 2023), clinical data (Harutyunyan et al., 2019), or computer vision (Ganin et al., 2016b).

**Domain adaptation.** Unsupervised Domain Adaptation (DA) addresses this problem by adapting a model trained on a labeled source dataset –or *domain*– so that it performs well on an unlabeled target domain, assuming some distribution shifts between the two (Ben-David et al., 2006; Quinonero-Candela et al., 2008; Redko et al., 2022). As illustrated in Figure 1, source and target distributions can exhibit various types of shifts (Moreno-Torres et al., 2012): changes in feature distributions (covariate shift), class proportions (target shift), conditional distributions (conditional shift), or in distributions in particular subspaces (subspace shift). Depending on the type of shift, existing DA methods attempt to align the source distribution closer to the target using reweighting (Sugiyama & Müller, 2005; Shimodaira, 2000), mapping (Sun et al., 2017; Courty et al., 2017b), or dimension reduction (Pan et al., 2011; Fernando et al., 2013) methods. More recently, it has been proposed to mitigate shifts in a feature space learned by deep learning (Ganin et al., 2016b; Sun & Saenko, 2016; Long et al., 2015a; Damodaran et al., 2018b), primarily focusing on computer vision applications. Regardless of the core algorithm used to address the domain shift, hyperparameters must be tuned for optimal performance. Indeed, a critical challenge in applying DA methods to real-world cases is selecting the appropriate method and tuning its hyperparameters, especially given the unknown shift type and the absence of labels in the target domain.

**Model selection in DA settings.** Without distribution shifts, classical model selection strategies –including hyperparameter optimization– rely on evaluating the generalization error with an independent labeled validation set. However, in DA, validating the hyperparameters in a supervised manner on the target domains is impossible due to the lack of labels. While it is possible to validate the hyperparameters on the source domain, it generally leads to a suboptimal model selection because of the distribution shift. In the literature, this problem is often raised but not always addressed. Some papers choose not to validate the parameters (Pan et al., 2011), while others validate on the source domain (Sun et al., 2017) or propose custom cross-validation methods (Sugiyama et al., 2007b). Few papers focus specifically on DA model selection criteria, which we will call *scorers* in this paper. These scorers are used to select the methods’ hyperparameters, and mainly consists of reweighting methods on source (Sugiyama et al., 2007a; You et al., 2019), prediction

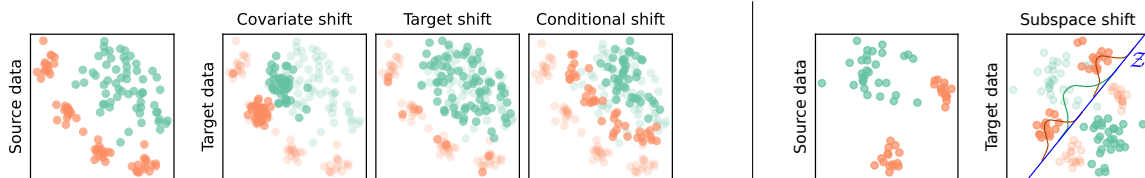


Figure 1: Illustration of the different data shifts and assumptions studied in the DA literature and used in the simulated datasets used in the numerical experiments. The colors indicate the classes, with solid colors representing target and transparent colors representing source in the target data plot.

entropy (Morerio et al., 2017; Saito et al., 2021) or circular validation (Bruzzone & Marconcini, 2010a). One of the goals of our benchmark is to evaluate these approaches in diverse and realistic scenarios.

**Benchmarks of DA.** As machine learning continues to flourish, new methods constantly emerge, making it essential to develop benchmarks that facilitate fair comparisons (Hutson, 2018; Pineau et al., 2019; Mattson et al., 2020; Moreau et al., 2022). In DA and related fields, several benchmarks have been proposed. Numerous papers focus on Out-of-distribution (OOD) datasets for different modalities: computer vision, text, graphs (Koh et al., 2021; Sagawa et al., 2022), time-series (Gagnon-Audet et al., 2023), AI-aided drug discovery (Ji et al., 2023) or tabular dataset (Gardner et al., 2023). Due to the type of data considered, existing benchmarks are mainly focused on Deep DA methods (Musgrave et al., 2021; Wang, 2018; Jiang et al., 2022; Fawaz et al., 2023), offering an incomplete evaluation of DA literature. Moreover, only a few benchmarks propose a comparison of Deep unsupervised DA methods with realistic parameters selection, on computer vision (Hu et al., 2023; Musgrave et al., 2021) and time series (Fawaz et al., 2023) data. Those benchmarks have shown the importance of validating with unsupervised scores and reveal that Deep DA methods achieve much lower performance in realistic scenarios.

**Contributions.** In the following, we propose **SKADA-Bench**, an ambitious and fully reproducible benchmark with the following features: **1.** A set of 4 simulated and 8 real-life datasets with different modalities (computer vision, NLP, tabular, biomedical) totaling 51 realistic shift scenarios, **2.** A wide range of 20 Shallow DA methods designed to handle different types of shifts, **3.** An evaluation of 3 deep DA methods on 4 real-world datasets from the computer vision and biomedical modalities, **4.** A realistic model selection procedure using 5 different unsupervised scorers with nested cross-validation for hyperparameter selection, **5.** An open-source implementation and publicly available datasets, easy to extend for new DA methods and datasets without the need to re-run the whole experiment.

In addition, we provide a detailed analysis of the results and derive guidelines for practitioners to select the best methods depending on the type of shifts, and the best scorer to perform unsupervised model selection. In particular, the effects of model selection and the scorer’s choice on the final performances are highlighted, showing a clear gap between the unsupervised realistic scorers versus using target labels for supervised validation.

## 2 Domain adaptation and model selection without target labels

In this section, we first discuss the specificities of the unsupervised domain adaptation problem and introduce several types of data shifts and their corresponding DA methods. Next, we discuss the different validation strategies used in the literature and the need for realistic scorers to compare DA methods.

### 2.1 Data shifts and DA strategies

**Domain Adaptation problem and theory.** The theoretical framework of DA is well established (Ben-David et al., 2006; Quinonero-Candela et al., 2008; Redko et al., 2022). The main results highlight that the performance discrepancy of an estimator between the source and target domains is linked to the divergence between both distributions. This has motivated the majority of DA methods to search for a universal (or domain invariant) predictor by minimizing the divergence between the two domains through the adaptation

of the distributions. This is done in practice by modeling and estimating the shift between the source and target distributions and then compensating for this shift before training a predictor.

**Data Shifts and DA methods.** A wide variety of shifts between the source and target distributions are possible. They are usually expressed as a relation between the joint distributions  $P^s(x, y) = P^s(x|y)P_y^s(y) = P^s(y|x)P_x^s(x)$  in the source domain and  $P^t(x, y) = P^t(x|y)P_y^t(y) = P^t(y|x)P_x^t(x)$  in the target domain. We now discuss the main types of shifts and the strategies proposed in the literature to mitigate them. Figure 1 illustrates these shifts.

In **Covariate shift** the conditionals probabilities are equal (*i.e.*,  $P^s(y|x) = P^t(y|x)$ ), but the feature marginals change (*i.e.*,  $P_x^s(x) \neq P_x^t(x)$ ). **Target shift** is similar, but the label marginals change  $P_y^s(y) \neq P_y^t(y)$  while the conditionals are preserved. For classification problems, it corresponds to a change in the proportion of the classes between the two domains. Both of those shifts can be compensated by **reweighting methods** that assign different weights to the samples of the source domain to make it closer to the target domain (Sugiyama & Müller, 2005; Shimodaira, 2000).

In **Conditional shift**, conditional probabilities differ between domain (*i.e.*,  $P^s(x|y) \neq P^t(x|y)$  or  $P^s(y|x) \neq P^t(y|x)$ ). This shift is typically harder to compensate for, necessitating explicit modeling to address it effectively. For instance, several approaches model the shift as a **mapping**  $m$  between the source and target domain such that  $P^s(y|m(x)) = P^t(y|x)$  (Sun et al., 2017; Courty et al., 2017b). The estimated mapping is then applied to the source data before training a predictor.

**Subspace shift** assumes that while probabilities are different between the domains ( $P_x^s(x) \neq P_x^t(x)$  and  $P^s(x|y) \neq P^t(x|y)$ ), there exists a subspace  $\mathcal{Z}$  and a function  $\phi : \mathcal{X} \rightarrow \mathcal{Z}$  such that  $P_{\mathcal{Z}}^s(\phi(x)) = P_{\mathcal{Z}}^t(\phi(x))$  and  $P^s(y|\phi(x)) = P^t(y|\phi(x))$ . Note that this means the shift occurs in the orthogonal complement of  $\mathcal{Z}$ . This implies that a classifier trained on  $\mathcal{Z}$  will perform well across both domains. **Subspace methods** are specifically designed towards identifying the subspace  $\mathcal{Z}$  and the function  $\phi$ , as developed in Pan et al. (2011); Fernando et al. (2013). Note that, as discussed in the introduction, a natural extension of this idea is to learn an invariant feature space using Deep learning (Ganin et al., 2016b; Sun & Saenko, 2016).

## 2.2 DA model selection strategies

As seen above, DA methods are typically designed to correct a specific type of shift. However, in real-world scenarios, the nature of the shift is often unknown. This presents a challenge in selecting the appropriate method and tuning its parameters when facing a new problem. In this section, we discuss the validation strategies proposed in the literature to compare DA methods, focusing on realistic scorers that do not use target labels.

**Realistic DA scorers.** In the literature, few papers propose realistic DA scorers to validate the parameters of the methods, *i.e.*, unsupervised scorers that **do not require target labels**. The *Importance Weighted (IW)* scorer (Sugiyama et al., 2007a) computes the score as a reweighted accuracy on labeled sources data. The *Deep Embedded Validation (DEV)* (You et al., 2019) can be seen as an IW in the latent space with a variance reduction strategy. DEV was originally proposed for Deep learning models but can be used on shallow DA methods that compute features from the data (mapping/subspaces). The *Prediction Entropy (PE)* scorer (Morero et al., 2017) measures the uncertainty associated with model predictions on the target data. *Soft Neighborhood Density (SND)* (Saito et al., 2021) also computes an entropy but on a normalized pairwise similarity matrix between probabilistic predictions on target. The *Circular Validation (CircV)* scorer (Bruzzone & Marconcini, 2010a) performs DA by first adapting the model from the source to the target domain and predicting the target labels. Next, it adapts back from the target to the source using these estimated labels. Performance is measured as the accuracy between the recovered and true source labels.

The *MixVal* scorer (Hu et al., 2023) also performs domain adaptation by first adapting the model from the source to the target domain and predicting the target labels. Then, it generates mixed target samples by probing intra-cluster samples to assess neighborhood density and inter-cluster samples to examine classification boundaries. The score is the accuracy between the generated targets labels and their predictions to evaluate the consistency.

**DA validation in the literature.** The model selection problem in DA has been widely discussed in the literature. Yet, this literature constitutes a subfield of DA and has seldom been used to validate new DA

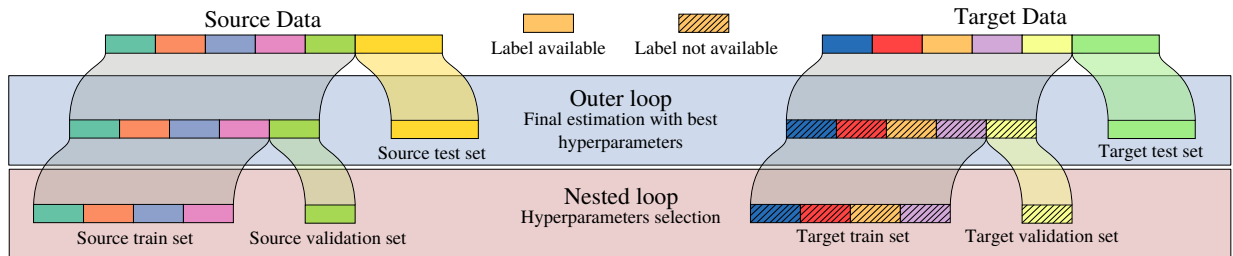


Figure 2: Visualization of nested cross-validation strategy. Both source and target data are split into an outer loop and then a nested loop. The nested loop tunes hyperparameters for the domain adaptation method, while the outer loop trains a final classifier with the best hyperparameters and evaluates its accuracy on both source and target data. Note: Target sets have no labels during the nested loop, reflecting unsupervised Domain Adaptation.

methods. Indeed, there is no consensus on the best validation strategy and many papers do not properly validate their methods, leading to over-estimated performances. Some authors do not discuss the validation procedure (Sugiyama & Müller, 2005; Shimodaira, 2000) or consider fixed hyperparameters (Huang et al., 2006). While some methods rely on custom validation techniques (Sugiyama et al., 2007b), others use cross-validation, either on the source or the target (Sun et al., 2017; Courty et al., 2017b), or alternatively other validation strategies proposed in the literature (Courty et al., 2017a; Bruzzone & Marconcini, 2010a). A complete picture of the model selection procedures used to validate the methods considered in *SKADA-Bench* in their original papers is presented in Table 4 in Appendix B. The goal of *SKADA-Bench* is therefore to constitute a dedicated benchmark to compare scorers from the literature and report performances that can be expected in real use cases for the considered methods.

### 3 A realistic benchmark for DA

In this section, we present our benchmark framework. First, we introduce the parameter validation strategies. Then, we present the compared DA methods followed by a description of the datasets used in the benchmark.

#### 3.1 Nested cross-validation loop and implementation

We discuss below the nested cross-validation and the implementation details of the benchmark.

**Hyperparameter validation loop.** We propose a nested loop cross-validation procedure, depicted in Figure 2. First, the source and target data are split into multiple outer test and train sets (outer loop in Figure 2). The test sets are kept to compute the final accuracy for both the source and target domains. For each split in the outer loop, we use a nested loop to select the DA methods’ parameters. Here, the training sets are further divided into nested train and validation sets (nested loop in Figure 2). Note that no labels are available for the target nested train and validation sets in this loop. The target training set is used to train the DA method, while the target validation set allows to compute the unsupervised score and select the best model.

For both loops, the data is split randomly 5 times using stratified sampling with an 80%/20% train/test split, except for Deep DA methods, where only one split is computed for the outer loop due to computation time. For one given method, we evaluate all the unsupervised scorers discussed earlier, as well as a supervised scorer that uses target labels, over all the nested splits. After averaging, the scores over the splits, the best hyperparameters are selected according to each scorer and then used to train a final classifier on the outer training sets. Although the supervised scorer cannot be used in practice, it is included in our results to actually evaluate the performance drop due to the absence of target labels. To limit complexity and perform a fair comparison of the methods, we set a timeout of 4 hours for performing the nested loop. Additionally, we chose not to use the *CircV* scorer for Deep DA methods, as training neural networks twice is computationally expensive.

---

**Base estimators and neural networks.** Existing shallow domain adaptation methods typically rely on either a base estimator trained on the adapted data or an iterative estimation process to adapt this estimator to the target data. The choice of the base estimator is crucial, as it significantly impacts the final performance. Before validating the hyperparameters of the DA methods, we determined the best estimator for each dataset using a grid-search on the source data. We tested multiple hyperparameters for Logistic Regression, SVM with RBF kernel, and XGBoost (Chen & Guestrin, 2016), selecting the ones that maximize the average accuracy on the source test sets. Note that for some methods that specifically require an SVM estimator (*i.e.*, JDOT and DASVM), we only validate SVM as the base estimator. We validated the base estimator separately from the DA methods parameters to reduce computational complexity and avoid too complex hyperparameter grids that can compromise the reliability of DA scorers. For Deep DA methods, we similarly select an appropriate architecture and experimental setup for training on the source data for each dataset: a two-layer convolutional neural network for MNIST/USPS, a ResNet50 (He et al., 2016) pretrained on ImageNet (Deng et al., 2009) for Office31 and Office Home, and a ShallowFBCSPNet (Schirrmester et al., 2017) for BCI. These architectures are widely used and well-supported in the literature of computer vision (Musgrave et al., 2021) and BCI (Schirrmester et al., 2017). During the nested loop, only the DA parameters for each method are validated.

**Best scorer selection and statistical test.** For all methods, we select the best validation scorer as the one that maximizes the averaged accuracy on the target domains for all real datasets. This provides a reasonable and actionable choice of scorer for each DA method for practitioners. For all methods and datasets, we perform a paired Wilcoxon signed-rank test at the 0.05 level to detect significant gain or drop in performance with respect to the no DA approach, denoted by “Train Src” in the following. The test is done using the accuracy measures of the DA method with the selected scorer and the Train Src for all shifts and outer splits, ensuring between 10 and 60 values depending on the dataset. Note that these statistical tests are not performed on Deep DA methods, as the number of splits is too limited for meaningful testing.

**Python implementation.** The benchmark code is available on GitHub upon publication of the paper.\* Our benchmark is implemented following the `benchopt` framework (Moreau et al., 2022), which provides standardized ways of organizing and running benchmarks for ML in Python. This framework facilitates reproducing the benchmark’s results, with tools to install the dependencies, run the methods in parallel, or cache the results to prevent redundant computations. It also makes it easy to extend the benchmark with additional datasets and methods, enabling it to evolve to account for the advances in the field. In the supplementary materials, we provide examples demonstrating how to add DA methods or datasets to the benchmark. Using this framework, we aim to make `SKADA-Bench` a reference benchmark to evaluate new DA methods in realistic scenarios with valid performance estimations.

### 3.2 Compared DA methods

In this section, we present the different families of domain adaptation methods that we compare in our benchmark. The shallow methods are grouped into four categories: reweighting methods, mapping methods, subspace methods, and others. For Deep DA methods, we consider three domain invariant feature methods. We provide a brief description of each method and the corresponding references.

**Reweighting methods.** These methods aim to reweight the source data to make it closer to the target data. The weights are estimated using different methods such as kernel density estimation (Dens. RW) (Sugiyama & Müller, 2005), Gaussian estimation (Gauss. RW) (Shimodaira, 2000), discriminative estimation (Discr. RW) (Shimodaira, 2000), or nearest-neighbors (NN RW) (Loog, 2012). Other reweighting estimate weights by minimizing a divergence between the source and target distributions such as Kullback-Leibler Importance Estimation Procedure (KLIEP) (Sugiyama et al., 2007b) or Kernel Mean Matching (KMM) (Huang et al., 2006). Finally, we also include the MMDTarS method (Zhang et al., 2013) that uses a Maximum Mean Discrepancy (MMD) to estimate the weights under the target shift hypothesis.

**Mapping methods.** These methods aim to find a mapping between the source and target data that minimizes the distribution shift. The Correlation Alignment method (CORAL) (Sun et al., 2017) aligns the second-order statistics of source and target distributions. The Maximum Mean Discrepancy (MMD-LS)

---

\*Our code is available in supplementary materials.

---

method (Zhang et al., 2013) minimizes the MMD to estimate an affine Location-Scale mapping. Finally, the Optimal Transport (OT) mapping methods (Courty et al., 2017b) use the optimal transport plan to align with a non-linear mapping of the source and target distributions with exact OT (MapOT), entropic regularization (EntOT), or class-based regularization (ClassRegOT). Finally, the Linear OT method (Flamary et al., 2020) uses a linear mapping to align the source and target distributions, assuming Gaussian distributions.

**Subspace methods.** These methods aim to learn a subspace where the source and target data have the same distribution. The Transfer Component Analysis (TCA) method (Pan et al., 2011) searches for a kernel embedding that minimizes the MMD divergence between the domains while preserving the variance. The Subspace Alignment (SA) method (Fernando et al., 2013) aims to learn a subspace where the source and target have their covariance matrices aligned. The Transfer Subspace Learning (TSL) method (Si et al., 2010) aims to learn a subspace using classical supervised loss functions on the source (*e.g.*, PCA, Fisher LDA) but regularized so that the source and target data have the same distribution once projected on the subspace. Finally, the Joint Principal Component Analysis (JPCA) method is a simple baseline that concatenates source and target data before applying a PCA.

**Others.** We also include other methods that do not fit into the previous categories. The Domain Adaptation SVM (DASVM) method (Bruzzone & Marconcini, 2010a) is a self-labeling method that iteratively updates SVM estimators by adding new target samples with predicted labels and removing source samples. The Joint Distribution Optimal Transport (JDOT) method (Courty et al., 2017a) aims to learn a target predictor that minimizes an OT loss between the joint source and target distributions. The Optimal Transport Label Propagation (OTLabelProp) method (Solomon et al., 2014) uses the optimal transport plan to propagate labels from the source to the target domain.

**Deep DA methods.** These methods aim to reduce the divergence between the source and target data distributions within the learned feature space while simultaneously learning a classifier on source data. The training loss consists in a traditional supervised loss on labeled source data and a second term measuring the discrepancy between the source and target distributions. The methods implemented in the Deep DA Benchmark use different discrepancies, such as covariance distance (Sun & Saenko, 2016) for DeepCORAL, adversarial loss (Ganin et al., 2016a) for DANN and optimal transport distance (Damodaran et al., 2018a) for DeepJDOT. Note that these approaches are not part of the main shallow DA benchmark but have been added to provide an interesting comparison of DA performances between shallow and Deep methods on computer vision and biomedical data.

### 3.3 Compared datasets

In this section, we present the datasets used in our experiments. We first introduce the synthetic datasets that implement different known shifts. Then, we describe the real-world datasets from various modalities and tasks such as Computer Vision (CV), Natural language Processing (NLP), tabular data, and biosignals.

**Simulated datasets.** The objective of the simulated datasets is to evaluate the performance of the DA methods under different types of shifts. Knowing that multiple DA methods have been built to handle specific shifts, evaluating them with this dataset will demonstrate whether they perform as expected and if they are properly validated.

The four simulated shifts in 2D, covariate (**Cov. shift**), target (**Tar. shift**) conditional (**Cond. shift**) and Subspace (**Sub. shift**) shift are illustrated in Figure 1. The source domain is represented by two non-linearly separable classes generated from one large and several smaller Gaussian blobs. In the experiments, the level of noise has been adjusted from Figure 1 to make the problem more difficult. For the subspace shift scenario, the source domain consists of one class represented by a large Gaussian blob and another class comprising Gaussian blobs positioned along the sides of the large one. The target domain is flipped along the diagonal, making the task challenging in the original space but feasible upon diagonal projection.

**Real-word datasets.** The real-world datasets used in our benchmark are summarized in Table 1. We select 8 datasets from different modalities and tasks: Computer Vision (CV) with **Office31** (Koniusz et al., 2017), **Office Home** (Venkateswara et al., 2017), and **MNIST/USPS** (Liao & Carneiro, 2015), Natural Language Processing (NLP) with **20Newsgroup** (Lang, 1995) and **Amazon Review** (McAuley et al., 2015), Tabular Data with **Mushrooms** (Dai et al., 2007) and **Phishing** (Mohammad et al., 2012), and Biosignals with **BCI**

Table 1: Characteristics of the real-world datasets used in SKADA-Bench.

Dataset	Modality	Preprocessing	# adapt	# classes	# samples	# features
Office 31 (Koniusz et al., 2017)	CV	Decaff + PCA (Donahue et al., 2014)	6	31	470 ± 350	100
Office Home (Venkateswara et al., 2017)	CV	ResNet + PCA (He et al., 2016)	12	65	3897 ± 850	100
MNIST/USPS (Liao & Carneiro, 2015)	CV	Vect + PCA	2	10	3000 / 10000	50
20 Newsgroup (Lang, 1995)	NLP	LLM + PCA (Reimers & Gurevych (2019), Xiao et al. (2023a))	6	2	3728 ± 174	50
Amazon Review (McAuley & Leskovec (2013), McAuley et al. (2015))	NLP	LLM + PCA (Reimers & Gurevych (2019), Xiao et al. (2023a))	12	4	2000	50
Mushrooms (Dai et al., 2007)	Tabular	One Hot Encoding	2	2	4062 ± 546	117
Phishing (Mohammad et al., 2012)	Tabular	NA	2	2	5527 ± 1734	30
BCI (Tangermann et al., 2012)	Biosignals	Cov+TS (Barachant et al., 2012)	9	4	288	253

Competition IV (Tangermann et al., 2012). The datasets are chosen to represent a wide range of shifts and to evaluate the performance of the methods on different types of data.

Before using shallow DA methods, the datasets are preprocessed with feature extraction to ensure reasonable performance when trained on each domain. For example, images are embedded using Deep pre-trained models followed by a PCA (except MNIST/USPS where only PCA is used), and textual data is embedded using Large Language Models (LLM) (Reimers & Gurevych, 2019; Xiao et al., 2023a) before applying a PCA. The tabular data are one-hot encoded to transform categorical data into numerical data. The biosignals from Brain-Computer Interface (BCI) data are embedded using the state-of-the-art tangent space representation proposed in Barachant et al. (2012). For Deep DA methods, only 4 datasets are used: Office31, Office Home, MNIST/USPS and BCI. Since these methods focus on learning feature representations, the data are used in their raw form. The datasets are split into pairs of source and target domains totaling 51 adaptation tasks in the benchmark. More details about the datasets and pre-processing are available in Appendix C.

## 4 Benchmark results

We now present the results of the benchmark. Training and evaluation across all shallow experiments required 1,215 CPU-hours on a standard Slurm (Yoo et al., 2003) cluster, while the Deep DA experiments required 244 GPU-hours. We first discuss and compare the performances of the methods on the different datasets. Then, a detailed study of the unsupervised scorers is provided.

### 4.1 Performance of the DA methods

**Results table.** First, we report the realistic performances of the different methods when using their selected scorer on the different datasets in Table 2. The cells showcasing a significant change in performance with the Wilcoxon test are highlighted with colors. Blue indicates an increase in performance, while red indicates a loss. The intensity of the color corresponds to the magnitude of the gain or loss - the darker the shade, the larger the positive or negative change. Cells with a NA values indicate that the method was not applicable to the dataset (DASVM is limited to binary classification) or that the method has reached a timeout. We also report the best scorer and the average rank of the methods for all real datasets. In addition to Table 2 providing realistic performance estimations with the best realistic scorer, we also report in Table 20 (Appendix E) the results when using the non-realistic supervised scorer.

**Simulated data with known shifts.** DA methods tend to show a significant gain on the shift they were designed for. It is especially true for mapping methods which greatly outperforms the Train Src approach under conditional shift (Cond. shift), almost reaching the Train Tgt performance for EntOT and ClassRegOT. The results also highlight that the mapping methods struggle with target shift (Tar. shift), which is a well-known limitation of this kind of approach (Redko et al., 2019). On the contrary, reweighting methods provide robust performance on target shift. Regarding covariate shift (Cov. shift), the improvement with reweighting

Table 2: Accuracy score for all datasets compared for all the shallow methods for simulated and real-life datasets. The color indicates the amount of the improvement. A white color means the method is not statistically different from Train Src (Train on source). Blue indicates that the score improved with the DA methods, while red indicates a decrease. The darker the color, the more significant the change.

		Cov. shift	Tar. shift	Concl. shift	Sub. shift	Office31	OfficeHome	MNIST/USPS	20NewsGroups	AmazonReview	Mushrooms	Phishing	BCI	Selected Scorer	Rank
	Train Src	0.88	0.85	0.66	0.19	0.65	0.56	0.54	0.59	0.7	0.72	0.91	0.55		10.66
	Train Tgt	0.92	0.93	0.82	0.98	0.89	0.8	0.96	1.0	0.73	1.0	0.97	0.64		1.55
Reweighting	Dens. RW	0.88	0.86	0.66	0.18	0.62	0.56	0.54	0.58	0.7	0.71	0.91	0.55	IW	12.20
	Disc. RW	0.85	0.83	0.71	0.18	0.63	0.54	0.5	0.6	0.68	0.75	0.91	0.56	CircV	8.75
	Gauss. RW	0.89	0.86	0.65	0.21	0.22	0.44	0.11	0.54	0.55	0.51	0.46	0.25	CircV	16.45
	KLIEP	0.88	0.86	0.66	0.19	0.65	0.56	0.54	0.6	0.69	0.72	0.91	0.55	CircV	10.56
	KMM	0.89	0.85	0.64	0.16	0.64	0.54	0.52	0.7	0.57	0.74	0.91	0.52	CircV	11.74
	NN RW	0.89	0.86	0.67	0.15	0.65	0.55	0.54	0.59	0.66	0.71	0.91	0.54	CircV	9.15
	MMDTarS	0.88	0.86	0.64	0.2	0.6	0.56	0.54	0.59	0.7	0.74	0.91	0.55	IW	10.81
Mapping	CORAL	0.74	0.7	0.76	0.18	0.65	0.57	0.62	0.73	0.7	0.72	0.92	0.62	CircV	5.08
	MapOT	0.72	0.57	0.82	0.02	0.6	0.51	0.61	0.76	0.68	0.63	0.84	0.47	PE	10.21
	EntOT	0.71	0.6	0.82	0.12	0.64	0.58	0.6	0.83	0.62	0.75	0.86	0.54	CircV	9.40
	ClassRegOT	0.74	0.58	0.81	0.11	NA	0.53	0.62	0.97	0.68	0.82	0.89	0.52	IW	8.25
	LinOT	0.73	0.73	0.76	0.18	0.66	0.57	0.64	0.82	0.7	0.76	0.91	0.61	CircV	4.06
	MMD-LS	0.78	0.72	0.76	0.56	0.65	0.56	0.55	0.97	0.63	0.85	NA	0.5	MixVal	8.22
Subspace	JPCA	0.88	0.85	0.66	0.15	0.62	0.48	0.51	0.77	0.69	0.78	0.9	0.54	PE	8.98
	SA	0.74	0.68	0.8	0.11	0.65	0.57	0.56	0.88	0.67	0.78	0.89	0.53	CircV	7.80
	TCA	0.52	0.47	0.51	0.62	0.04	0.02	0.07	0.61	0.61	0.49	0.48	0.26	DEV	17.58
	TSL	0.88	0.85	0.66	0.2	0.63	0.48	0.45	0.63	0.69	0.45	0.89	0.26	IW	15.09
Other	JDOT	0.72	0.58	0.82	0.13	0.6	0.42	0.59	0.79	0.67	0.65	0.79	0.47	IW	11.42
	OTLabelProp	0.72	0.59	0.8	0.07	0.66	0.56	0.62	0.86	0.67	0.64	0.86	0.5	CircV	10.01
	DASVM	0.89	0.86	0.65	0.15	NA	NA	NA	0.87	NA	0.83	0.85	NA	MixVal	7.29

methods is very limited although reweighting is specifically designed for this kind of shift. We believe that using a complex base estimator (here an SVM with an RBF kernel) enables us to train an estimator that works well on both source and target, reducing the impact of importance weighting as previously highlighted in (Byrd & Lipton, 2019) for deep neural networks. The results reported in Table 17 of Appendix E reveal that reweighting methods significantly outperform Train Src when using a linear base classifier.

**Real data with unknown shift.** *The performance of reweighting methods is often close to Train Src baseline on real datasets.* This result can be due to the violations of the same-support assumption, which is crucial for reweighting to work effectively (Segovia-Martín et al., 2023) which is likely true for the three CV datasets. In this case, hyperparameter tuning frequently select configurations leading to near-uniform weighting, which explain the close performance to Train Src.

*The performance of mapping methods is dataset-dependent, potentially due to the number of classes and presence of target shift.* Mapping methods excel on MNIST/USPS and 20NewsGroup which respectively contain 10 and 2 classes, but failing on Office31 and OfficeHome with 31 and 60 classes. Additionally, while mapping performs well on the NLP dataset 20NewsGroup, it results in negative transfer on Amazon Reviews which has target shifts.

*It is notable that simple transformations are the best in average across all modalities.* Indeed most methods that significantly outperform Train Src in ranking average across all modalities are LinOT, CORAL, JPCA, and SA, which all rely on linear transformations such as scaling, linear projection or rotations. These methods are robust across datasets and modalities, offering effective alignment with minimal risk of negative DA.

**Take-away for DA users.** Reweighting methods are best suited for scenarios where the same-support assumption holds and perform particularly well when paired with regularized hypotheses like linear models.

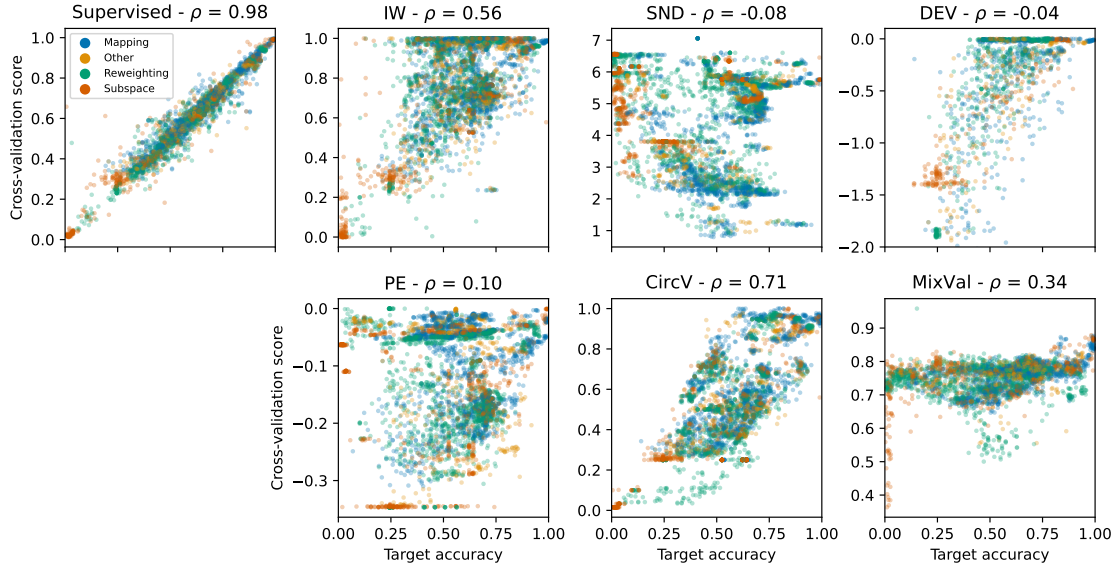


Figure 3: Cross-val score as a function of the accuracy for different supervised and unsupervised scorers. The Pearson correlation coefficient is reported for each scorer by  $\rho$ . Each point represents an inner split with a DA method (color of the points) and a dataset. A good score should correlate with the target accuracy.

Even when assumptions are not fully satisfied, reweighting tends to be robust to negative transfer. Mapping methods are highly effective under moderate numbers of classes and in the absence of target shift but carry a significant risk of negative transfer if target shift is present. When the type of distribution shift is uncertain, simpler transformation-based methods like LinOT, CoRAL, JPCA, and SA provide modest performance improvements while minimizing risks of negative DA, making them reliable and safe default options.

**Selected scorer per DA method.** We observe that the best scorer differs across methods, Circular Validation has been selected 10 out of 20 times as the best scorer, followed by Importance Weighting 4 out of 20 times. Table 20 in the supplementary material provides the non-realistic accuracy results with the supervised scorer. It is worth noting that the supervised scorer generally outperforms the unsupervised ones, and several methods significantly outperform Train Src in each dataset. It is crucial to choose the model realistically to avoid producing overly optimistic results, as many data analysis papers have done (see Table 4).

These results show the methods’ sensitivity to parameter selections and the difficulty of using realistic scorers. This might also explain why DA methods are not widely used in practice: they are very difficult to tune and might decrease performances compared with no adaptation.

## 4.2 Study of validation scorers

We now investigate the performance of the various scorers to select hyperparameters of the DA method. First, we consider the relationship between the cross-val score and the accuracy for each inner split. In Figure 3, we plot for each scorer the cross-val score as a function of the accuracy computed on the test set and report the Pearson correlation coefficient  $\rho$ . As expected, the supervised scorer is highly correlated with the accuracy ( $\rho = 0.98$ ), as it has access to the target labels. We observe that SND, DEV, and PE do not provide a good proxy to select hyperparameters that give the best-performing models ( $\rho \leq 0.06$ ). On the contrary, MixVal, IW and CircV are correlated with the accuracy,  $\rho = 0.34$ ,  $\rho = 0.56$  and  $\rho = 0.71$  respectively. This is coherent with their selection as the best scorer in most scenarios in Table 2. Still, while those scorers are well correlated with the target accuracy, it is important to note that they have a large variance. For instance, a score close to 1 in IW or CircV corresponds to an accuracy between 0.5 and 1.0.

Furthermore, we provide in Figures 8 and 9, from Appendix E, several visualizations that illustrate the relationship between the accuracy achieved when using a supervised scorer and the accuracy obtained when using different unsupervised scorers. We also visualize in Figure 7 the drop in performance when using the

best-unsupervised scorer instead of the supervised scorer. Interestingly some methods such as KMM, EntOT, and ClassRegOT can lose up to 10% accuracy when using realistic scorers, which might come from their higher number of parameters or their sensitivity to them.

Our results thus show that most scorers have poor results when evaluated on many datasets. Of the five methods under consideration, only two achieve satisfactory performance, although incurring large variance in their results. This shows that proper hyperparameter selection is still an open question, that needs attention from the research community to guide practitioners toward real life applications of unsupervised DA technics.

### 4.3 Deep DA methods

Although most of the recent work on domain adaptation focus on Deep methods for computer vision tasks, shallow methods are competitive in many applications such as tabular data (Grinsztajn et al., 2022) or datasets with a relatively small number of training examples such as BCI (Chevalier et al., 2024). Moreover, shallow methods can also benefit from recent advances in Deep learning by using Deep pre-trained feature extraction (transfer learning). However, to the best of our knowledge,

the literature lacks quantitative comparison between shallow methods applied on Deep pre-trained feature extraction and Deep DA methods. To this end, we ran a benchmark using the same pipeline as in Table 2 with three Domain Invariant Deep DA methods on the CV and BCI datasets.

The results are available in Table 3 with a comparison to the best performing shallow method from Table 2. One of the most notable and expected difference is on MNIST/USPS. Shallow methods struggle to achieve good performances, even on Train Tgt, as they rely on PCA for feature extraction. Deep methods, on the other hand, use CNNs, leading to large accuracy gains on train on Src and Tgt but also on Deep DA methods. However, it is important to note that while DeepJDOT, DANN and MCC improve performance on all datasets, they remain far from the train on Tgt accuracies, partly due to the difficulty in tuning their parameters (see Appendix E.3 with the supervised scorer). The superior performance of Deep DA methods on CV datasets can be attributed to the relationship between classification in the DA subspace and the disentanglement of semantic (discriminant) content from style (domain shift) (Gonzalez-Garcia et al., 2018; Gabbay et al., 2021). Numerous studies have demonstrated that semantic embeddings can be effectively recovered, supporting the assumption that a (nonlinear) subspace shift is reasonable for CV tasks. However, for the BCI dataset, where the amount of data is limited, the performances of Deep DA methods are inferior to some other shallow methods (*i.e.*, LinOT for example). Finally, a method like DANN, which is often considered as a baseline in the community, has been shown to be hard to validate and requires setup that can be difficult to determine across different settings. These results emphasize, that while Deep invariant DA methods can be effective, they do not consistently yield good results across modalities, whereas shallow DA methods can achieve similar or superior performances with less effort and fewer computational resources in low data regimes.

## 5 Conclusion

In this work, we introduced **SKADA-Bench**, a extensive benchmark for unsupervised domain adaptation, carefully evaluating the impact of the model selection criteria and covering diverse modalities: computer

Table 3: Accuracy scores for Deep methods on selected real-life datasets using DA scorers. LinOT is reported as the overall top-performing shallow method. Green indicates that the score improved with the DA methods. The darker the color, the more significant the change.

	MNIST/USPS	Office31	OfficeHome	BCI	Selected Scorer	Rank
Train Src	0.85	0.77	0.58	0.54		6.19
Train Tgt	0.98	0.96	0.83	0.56		2.07
DeepCORAL (Sun & Saenko, 2016)	0.93	0.77	0.59	0.54	MixVal	3.29
DAN (Long et al., 2015b)	0.86	0.75	0.56	0.53	IW	4.76
DANN (Ganin et al., 2016a)	0.9	0.79	0.59	0.41	MixVal	4.98
DeepJDOT (Damodaran et al., 2018b)	0.9	0.82	0.62	0.54	PE	2.92
MCC (Jin et al., 2020)	0.93	0.83	0.66	0.53	MixVal	2.38
MDD (Zhang et al., 2019)	0.87	0.78	0.56	0.4	MixVal	4.96
SPA (Xiao et al., 2023b)	0.91	0.78	0.56	0.41	DEV	5.39
LinOT (Flamary et al., 2020)	0.64	0.6	0.57	0.61	CircV	

---

vision, natural language processing, tabular data and biosignals. While being quite comprehensive on shallow methods, our results also provide a comparison of three common deep DA baselines on computer vision and biosignals. Importantly **SKADA-Bench** can be easily extended with new datasets and methods to push further the state-of-the-art. Our findings reveal that few shallow DA methods consistently perform well across diverse datasets and that model selection scorers significantly influence their effectiveness. While deep DA methods show similar trends, they often require more extensive hyperparameter tuning and architectures tailored to each modality. Notably, they tend to perform significantly better than shallow methods on some modalities, such as computer vision, while facing challenges on others such as biosignals. For each DA method, we provide the optimal model selection scorer for unsupervised hyperparameter tuning based on our experiments.

## Acknowledgments

This work was supported by grant ANR-22-PESN-0012 to AC under the France 2030 program, ANR-20-CHIA-0016 and ANR-20-IADJ-0002 to AG, and ANR-23-ERCC-0006 to YL, TG, and RF, all managed by the Agence Nationale de la Recherche (ANR). Additionally, this project received funding from the European Union’s Horizon Europe research and innovation program under grant agreement 101120237 (ELIAS).

All the datasets used for this work were accessed and processed on the Inria and IP Paris (IDCS) compute infrastructures.

## References

- Bruno Aristimunha, Igor Carrara, Pierre Guetschel, Sara Sedlar, Pedro Rodrigues, Jan Sosulski, Divyesh Narayanan, Erik Bjareholt, Barthelemy Quentin, Robin Tibor Schirmer, Emmanuel Kalunga, Ludovic Darnet, Cattan Gregoire, Ali Abdul Hussain, Ramiro Gatti, Vladislav Goncharenko, Jordy Thielen, Thomas Moreau, Yannick Roy, Vinay Jayaram, Alexandre Barachant, and Sylvain Chevallier. Mother of all bci benchmarks v0.5. [doi.org/10.5281/zenodo.10034223](https://doi.org/10.5281/zenodo.10034223), 2023. DOI: 10.5281/zenodo.10034223.
- Alexandre Barachant, Stéphane Bonnet, Marco Congedo, and Christian Jutten. Multiclass brain-computer interface classification by riemannian geometry. *IEEE Transactions on Biomedical Engineering*, 59(4): 920–928, 2012. doi: 10.1109/TBME.2011.2172210.
- Shai Ben-David, John Blitzer, Koby Crammer, and Fernando Pereira. Analysis of representations for domain adaptation. In B. Schölkopf, J. Platt, and T. Hoffman (eds.), *Advances in Neural Information Processing Systems*, volume 19. MIT Press, 2006. URL [https://proceedings.neurips.cc/paper\\_files/paper/2006/file/b1b0432ceafb0ce714426e9114852ac7-Paper.pdf](https://proceedings.neurips.cc/paper_files/paper/2006/file/b1b0432ceafb0ce714426e9114852ac7-Paper.pdf).
- Lorenzo Bruzzone and Mattia Marconcini. Domain adaptation problems: A dasvm classification technique and a circular validation strategy. *IEEE Transactions on Pattern Analysis and Machine Intelligence*, 32(5): 770–787, 2010a. doi: 10.1109/TPAMI.2009.57.
- Lorenzo Bruzzone and Mattia Marconcini. Domain adaptation problems: A dasvm classification technique and a circular validation strategy. *IEEE Transactions on Pattern Analysis and Machine Intelligence*, 32(5): 770–787, 2010b. doi: 10.1109/TPAMI.2009.57.
- Jonathon Byrd and Zachary Lipton. What is the effect of importance weighting in deep learning? In *International conference on machine learning*, pp. 872–881. PMLR, 2019.
- Tianqi Chen and Carlos Guestrin. Xgboost: A scalable tree boosting system. In *Proceedings of the 22nd acm sigkdd international conference on knowledge discovery and data mining*, pp. 785–794, 2016.
- Sylvain Chevallier, Igor Carrara, Bruno Aristimunha, Pierre Guetschel, Sara Sedlar, Bruna Lopes, Sebastien Velut, Salim Khazem, and Thomas Moreau. The largest eeg-based bci reproducibility study for open science: the moabb benchmark. *arXiv preprint arXiv:2404.15319*, 2024.
- Nicolas Courty, Rémi Flamary, Amaury Habrard, and Alain Rakotomamonjy. Joint distribution optimal transportation for domain adaptation. In I. Guyon, U. Von Luxburg, S. Bengio, H. Wallach, R. Fergus,

- 
- S. Vishwanathan, and R. Garnett (eds.), *Advances in Neural Information Processing Systems*, volume 30. Curran Associates, Inc., 2017a. URL [https://proceedings.neurips.cc/paper\\_files/paper/2017/file/0070d23b06b1486a538c0eaa45dd167a-Paper.pdf](https://proceedings.neurips.cc/paper_files/paper/2017/file/0070d23b06b1486a538c0eaa45dd167a-Paper.pdf).
- Nicolas Courty, Rémi Flamary, Devis Tuia, and Alain Rakotomamonjy. Optimal transport for domain adaptation. *IEEE Transactions on Pattern Analysis and Machine Intelligence*, 39(9):1853–1865, 2017b. doi: 10.1109/TPAMI.2016.2615921.
- Wenyuan Dai, Qiang Yang, Gui-Rong Xue, and Yong Yu. Boosting for transfer learning. In *Proceedings of the 24th International Conference on Machine Learning, ICML '07*, pp. 193–200, New York, NY, USA, 2007. Association for Computing Machinery. ISBN 9781595937933. doi: 10.1145/1273496.1273521. URL <https://doi.org/10.1145/1273496.1273521>.
- Bharath Bhushan Damodaran, Benjamin Kellenberger, Rémi Flamary, Devis Tuia, and Nicolas Courty. Deepjdot: Deep joint distribution optimal transport for unsupervised domain adaptation. In *European Conference on Computer Vision*, 2018a. URL <https://api.semanticscholar.org/CorpusID:4331539>.
- Bharath Bhushan Damodaran, Benjamin Kellenberger, Rémi Flamary, Devis Tuia, and Nicolas Courty. Deepjdot: Deep joint distribution optimal transport for unsupervised domain adaptation. In *Computer Vision – ECCV 2018: 15th European Conference, Munich, Germany, September 8-14, 2018, Proceedings, Part IV*, pp. 467–483, Berlin, Heidelberg, 2018b. Springer-Verlag. ISBN 978-3-030-01224-3. doi: 10.1007/978-3-030-01225-0\_28. URL [https://doi.org/10.1007/978-3-030-01225-0\\_28](https://doi.org/10.1007/978-3-030-01225-0_28).
- Jia Deng, Wei Dong, Richard Socher, Li-Jia Li, Kai Li, and Li Fei-Fei. Imagenet: A large-scale hierarchical image database. In *2009 IEEE conference on computer vision and pattern recognition*, pp. 248–255. Ieee, 2009.
- Jeff Donahue, Yangqing Jia, Oriol Vinyals, Judy Hoffman, Ning Zhang, Eric Tzeng, and Trevor Darrell. Decaf: A deep convolutional activation feature for generic visual recognition. In Eric P. Xing and Tony Jebara (eds.), *Proceedings of the 31st International Conference on Machine Learning*, volume 32 of *Proceedings of Machine Learning Research*, pp. 647–655, Beijing, China, 22–24 Jun 2014. PMLR. URL <https://proceedings.mlr.press/v32/donahue14.html>.
- Hassan Ismail Fawaz, Ganesh Del Grosso, Tanguy Kerdoncuff, Aurelie Boisbunon, and Illyne Saffar. Deep unsupervised domain adaptation for time series classification: a benchmark. *arXiv preprint arXiv:2312.09857*, 2023.
- Basura Fernando, Amaury Habrard, Marc Sebban, and Tinne Tuytelaars. Unsupervised visual domain adaptation using subspace alignment. In *2013 IEEE International Conference on Computer Vision*, pp. 2960–2967, 2013. doi: 10.1109/ICCV.2013.368.
- Rémi Flamary, Karim Lounici, and André Ferrari. Concentration bounds for linear monge mapping estimation and optimal transport domain adaptation, 2020.
- Aviv Gabbay, Niv Cohen, and Yedid Hoshen. An image is worth more than a thousand words: Towards disentanglement in the wild. *Advances in Neural Information Processing Systems*, 34:9216–9228, 2021.
- Jean-Christophe Gagnon-Audet, Kartik Ahuja, Mohammad Javad Darvishi Bayazi, Pooneh Mousavi, Guillaume Dumas, and Irina Rish. WOODS: Benchmarks for out-of-distribution generalization in time series. *Transactions on Machine Learning Research*, 2023. ISSN 2835-8856. URL <https://openreview.net/forum?id=mvftzofTYQ>. Featured Certification.
- Yaroslav Ganin, Evgeniya Ustinova, Hana Ajakan, Pascal Germain, Hugo Larochelle, François Laviolette, Mario March, and Victor Lempitsky. Domain-adversarial training of neural networks. *Journal of machine learning research*, 17(59):1–35, 2016a.
- Yaroslav Ganin, Evgeniya Ustinova, Hana Ajakan, Pascal Germain, Hugo Larochelle, François Laviolette, Mario March, and Victor Lempitsky. Domain-adversarial training of neural networks. *Journal of Machine Learning Research*, 17(59):1–35, 2016b. URL <http://jmlr.org/papers/v17/15-239.html>.

- 
- Joshua P Gardner, Zoran Popovi, and Ludwig Schmidt. Benchmarking distribution shift in tabular data with tableshift. In *Thirty-seventh Conference on Neural Information Processing Systems Datasets and Benchmarks Track*, 2023. URL <https://openreview.net/forum?id=XYxNklOMMX>.
- Théo Gnassounou, Oleksii Kachaiev, Rémi Flamary, Antoine Collas, Yanis Lalou, Antoine Mathelin, Alexandre Gramfort, Ruben Bueno, Florent Michel, Apolline Mellot, Virginie Loison, Ambroise Odonnat, and Thomas Moreau. Skada : Scikit adaptation, July 2024. URL <https://doi.org/10.5281/zenodo.12666838>.
- Abel Gonzalez-Garcia, Joost Van De Weijer, and Yoshua Bengio. Image-to-image translation for cross-domain disentanglement. *Advances in neural information processing systems*, 31, 2018.
- Léo Grinsztajn, Edouard Oyallon, and Gaël Varoquaux. Why do tree-based models still outperform deep learning on typical tabular data? *Advances in neural information processing systems*, 35:507–520, 2022.
- Hrayr Harutyunyan, Hrant Khachatryan, David C. Kale, Greg Ver Steeg, and Aram Galstyan. Multitask learning and benchmarking with clinical time series data. *Scientific Data*, 6(1), June 2019. ISSN 2052-4463. doi: 10.1038/s41597-019-0103-9. URL <http://dx.doi.org/10.1038/s41597-019-0103-9>.
- Kaiming He, Xiangyu Zhang, Shaoqing Ren, and Jian Sun. Deep residual learning for image recognition. In *2016 IEEE Conference on Computer Vision and Pattern Recognition (CVPR)*, pp. 770–778, 2016. doi: 10.1109/CVPR.2016.90.
- Dapeng Hu, Jian Liang, Jun Hao Liew, Chuhui Xue, Song Bai, and Xinchao Wang. Mixed samples as probes for unsupervised model selection in domain adaptation. In A. Oh, T. Naumann, A. Globerson, K. Saenko, M. Hardt, and S. Levine (eds.), *Advances in Neural Information Processing Systems*, volume 36, pp. 37923–37941. Curran Associates, Inc., 2023. URL [https://proceedings.neurips.cc/paper\\_files/paper/2023/file/7721f1fea280e9ffae528dc78c732576-Paper-Conference.pdf](https://proceedings.neurips.cc/paper_files/paper/2023/file/7721f1fea280e9ffae528dc78c732576-Paper-Conference.pdf).
- Jiayuan Huang, Arthur Gretton, Karsten Borgwardt, Bernhard Schölkopf, and Alex Smola. Correcting sample selection bias by unlabeled data. In B. Schölkopf, J. Platt, and T. Hoffman (eds.), *Advances in Neural Information Processing Systems*, volume 19. MIT Press, 2006. URL [https://proceedings.neurips.cc/paper\\_files/paper/2006/file/a2186aa7c086b46ad4e8bf81e2a3a19b-Paper.pdf](https://proceedings.neurips.cc/paper_files/paper/2006/file/a2186aa7c086b46ad4e8bf81e2a3a19b-Paper.pdf).
- Matthew Hutson. Artificial intelligence faces reproducibility crisis, 2018.
- Yuanfeng Ji, Lu Zhang, Jiaxiang Wu, Bingzhe Wu, Lanqing Li, Long-Kai Huang, Tingyang Xu, Yu Rong, Jie Ren, Ding Xue, Houtim Lai, Wei Liu, Junzhou Huang, Shuigeng Zhou, Ping Luo, Peilin Zhao, and Yatao Bian. Drugood: Out-of-distribution dataset curator and benchmark for ai-aided drug discovery – a focus on affinity prediction problems with noise annotations. *Proceedings of the AAAI Conference on Artificial Intelligence*, 37(7):8023–8031, Jun. 2023. doi: 10.1609/aaai.v37i7.25970. URL <https://ojs.aaai.org/index.php/AAAI/article/view/25970>.
- Junguang Jiang, Yang Shu, Jianmin Wang, and Mingsheng Long. Transferability in deep learning: A survey, 2022.
- Ying Jin, Ximei Wang, Mingsheng Long, and Jianmin Wang. Minimum class confusion for versatile domain adaptation, 2020. URL <https://arxiv.org/abs/1912.03699>.
- Pang Wei Koh, Shiori Sagawa, Henrik Marklund, Sang Michael Xie, Marvin Zhang, Akshay Balsubramani, Weihua Hu, Michihiro Yasunaga, Richard Lanus Phillips, Irena Gao, Tony Lee, Etienne David, Ian Stavness, Wei Guo, Berton Earnshaw, Imran Haque, Sara M Beery, Jure Leskovec, Anshul Kundaje, Emma Pierson, Sergey Levine, Chelsea Finn, and Percy Liang. Wilds: A benchmark of in-the-wild distribution shifts. In Marina Meila and Tong Zhang (eds.), *Proceedings of the 38th International Conference on Machine Learning*, volume 139 of *Proceedings of Machine Learning Research*, pp. 5637–5664. PMLR, 18–24 Jul 2021. URL <https://proceedings.mlr.press/v139/koh21a.html>.
- Piotr Koniusz, Yusuf Tas, and Fatih Porikli. Domain adaptation by mixture of alignments of second-order higher-order scatter tensors. In *2017 IEEE Conference on Computer Vision and Pattern Recognition (CVPR)*, pp. 7139–7148, 2017. doi: 10.1109/CVPR.2017.755.

- 
- Ken Lang. Newsweeder: Learning to filter netnews. In *Proceedings of the Twelfth International Conference on Machine Learning*, pp. 331–339, 1995.
- Zhibin Liao and Gustavo Carneiro. Competitive multi-scale convolution, 2015.
- Mingsheng Long, Yue Cao, Jianmin Wang, and Michael Jordan. Learning transferable features with deep adaptation networks. In Francis Bach and David Blei (eds.), *Proceedings of the 32nd International Conference on Machine Learning*, volume 37 of *Proceedings of Machine Learning Research*, pp. 97–105, Lille, France, 07–09 Jul 2015a. PMLR. URL <https://proceedings.mlr.press/v37/long15.html>.
- Mingsheng Long, Yue Cao, Jianmin Wang, and Michael I. Jordan. Learning transferable features with deep adaptation networks, 2015b. URL <https://arxiv.org/abs/1502.02791>.
- M Loog. Nearest neighbor-based importance weighting. In SN (ed.), *The 2012 IEEE workshop on machine learning for signal processing (MLSP) proceedings*, pp. 1–6, United States, 2012. IEEE. ISBN 978-1-4673-1026-0/12. The 2012 IEEE workshop on machine learning for signal processing (MLSP) ; Conference date: 23-09-2012 Through 26-09-2012.
- Peter Mattson, Vijay Janapa Reddi, Christine Cheng, Cody Coleman, Greg Diamos, David Kanter, Paulius Micikevicius, David Patterson, Guenther Schmuelling, Hanlin Tang, Gu-Yeon Wei, and Carole-Jean Wu. Mlperf: An industry standard benchmark suite for machine learning performance. *IEEE Micro*, 40(2):8–16, 2020. doi: 10.1109/MM.2020.2974843.
- Julian McAuley and Jure Leskovec. Hidden factors and hidden topics: understanding rating dimensions with review text. In *Proceedings of the 7th ACM conference on Recommender systems*, pp. 165–172, 2013.
- Julian McAuley, Christopher Targett, Qinfeng Shi, and Anton van den Hengel. Image-based recommendations on styles and substitutes. In *Proceedings of the 38th International ACM SIGIR Conference on Research and Development in Information Retrieval*, SIGIR ’15, pp. 43–52, New York, NY, USA, 2015. Association for Computing Machinery. ISBN 9781450336215. doi: 10.1145/2766462.2767755. URL <https://doi.org/10.1145/2766462.2767755>.
- Rami M. Mohammad, Fadi Thabtah, and Lee McCluskey. An assessment of features related to phishing websites using an automated technique. In *2012 International Conference for Internet Technology and Secured Transactions*, pp. 492–497, 2012.
- Thomas Moreau, Mathurin Massias, Alexandre Gramfort, Pierre Ablin, Pierre-Antoine Bannier, Benjamin Charlier, Mathieu Dagr eou, Tom Dupre la Tour, Ghislain Durif, C assio Fraga Dantas, Quentin Klopfenstein, Johan Larsson, En Lai, Tanguy Lefort, Beno t Mal ezieux, Badr Moufad, Binh Nguyen, Alain Rakotomamonjy, Zaccharie Ramzi, Joseph Salmon, and Samuel Vaiter. Benchopt: Reproducible, efficient and collaborative optimization benchmarks. In Alice H. Oh, Alekh Agarwal, Danielle Belgrave, and Kyunghyun Cho (eds.), *Advances in Neural Information Processing Systems*, 2022. URL <https://openreview.net/forum?id=1uSzacpyWLH>.
- Jose G. Moreno-Torres, Troy Raeder, Roc o Alaiz-Rodr iguez, Nitesh V. Chawla, and Francisco Herrera. A unifying view on dataset shift in classification. *Pattern Recognition*, 45(1):521–530, January 2012. doi: 10.1016/j.patcog.2011.06.019.
- Pietro Morerio, Jacopo Cavazza, and Vittorio Murino. Minimal-entropy correlation alignment for unsupervised deep domain adaptation, 2017.
- Kevin Musgrave, Serge Belongie, and Ser-Nam Lim. Unsupervised domain adaptation: A reality check. *arXiv preprint arXiv:2111.15672*, 2021.
- Sinno Jialin Pan, Ivor W. Tsang, James T. Kwok, and Qiang Yang. Domain adaptation via transfer component analysis. *IEEE Transactions on Neural Networks*, 22(2):199–210, 2011. doi: 10.1109/TNN.2010.2091281.
- Joelle Pineau, Koustuv Sinha, Genevieve Fried, Rosemary Nan Ke, and Hugo Larochelle. Iclr reproducibility challenge 2019. *ReScience C*, 5(2):5, 2019.

- 
- Joaquin Quinonero-Candela, Masashi Sugiyama, Anton Schwaighofer, and Neil D Lawrence. *Dataset shift in machine learning*. MIT Press, 2008.
- Ievgen Redko, Nicolas Courty, Rémi Flamary, and Devis Tuia. Optimal transport for multi-source domain adaptation under target shift. In *The 22nd International Conference on artificial intelligence and statistics*, pp. 849–858. PMLR, 2019.
- Ievgen Redko, Emilie Morvant, Amaury Habrard, Marc Sebban, and Younès Bennani. A survey on domain adaptation theory: learning bounds and theoretical guarantees, 2022.
- Nils Reimers and Iryna Gurevych. Sentence-bert: Sentence embeddings using siamese bert-networks. In Kentaro Inui, Jing Jiang, Vincent Ng, and Xiaojun Wan (eds.), *EMNLP/IJCNLP (1)*, pp. 3980–3990. Association for Computational Linguistics, 2019. ISBN 978-1-950737-90-1. URL <http://dblp.uni-trier.de/db/conf/emnlp/emnlp2019-1.html#ReimersG19>.
- Shiori Sagawa, Pang Wei Koh, Tony Lee, Irena Gao, Sang Michael Xie, Kendrick Shen, Ananya Kumar, Weihua Hu, Michihiro Yasunaga, Henrik Marklund, Sara Beery, Etienne David, Ian Stavness, Wei Guo, Jure Leskovec, Kate Saenko, Tatsunori Hashimoto, Sergey Levine, Chelsea Finn, and Percy Liang. Extending the WILDS benchmark for unsupervised adaptation. In *International Conference on Learning Representations*, 2022. URL <https://openreview.net/forum?id=z7p2V6KR00V>.
- Kuniaki Saito, Donghyun Kim, Piotr Teterwak, Stan Sclaroff, Trevor Darrell, and Kate Saenko. Tune it the right way: Unsupervised validation of domain adaptation via soft neighborhood density. In *2021 IEEE/CVF International Conference on Computer Vision (ICCV)*, pp. 9164–9173, 2021. doi: 10.1109/ICCV48922.2021.00905.
- Robin Tibor Schirrmeyer, Jost Tobias Springenberg, Lukas Dominique Josef Fiederer, Martin Glasstetter, Katharina Eggensperger, Michael Tangermann, Frank Hutter, Wolfram Burgard, and Tonio Ball. Deep learning with convolutional neural networks for eeg decoding and visualization. *Human brain mapping*, 38(11):5391–5420, 2017.
- José I Segovia-Martín, Santiago Mazuelas, and Anqi Liu. Double-weighting for covariate shift adaptation. In *International Conference on Machine Learning*, pp. 30439–30457. PMLR, 2023.
- Hidetoshi Shimodaira. Improving predictive inference under covariate shift by weighting the log-likelihood function. *Journal of Statistical Planning and Inference*, 90(2):227–244, 2000. ISSN 0378-3758. doi: [https://doi.org/10.1016/S0378-3758\(00\)00115-4](https://doi.org/10.1016/S0378-3758(00)00115-4). URL <https://www.sciencedirect.com/science/article/pii/S0378375800001154>.
- Si Si, Dacheng Tao, and Bo Geng. Bregman divergence-based regularization for transfer subspace learning. *IEEE Transactions on Knowledge and Data Engineering*, 22(7):929–942, 2010. doi: 10.1109/TKDE.2009.126.
- Justin Solomon, Raif Rustamov, Leonidas Guibas, and Adrian Butscher. Wasserstein propagation for semi-supervised learning. In Eric P. Xing and Tony Jebara (eds.), *Proceedings of the 31st International Conference on Machine Learning*, volume 32 of *Proceedings of Machine Learning Research*, pp. 306–314, Beijing, China, 22–24 Jun 2014. PMLR. URL <https://proceedings.mlr.press/v32/solomon14.html>.
- Masashi Sugiyama and Klaus-Robert Müller. Input-dependent estimation of generalization error under covariate shift. *Statistics & Risk Modeling*, 23(4):249–279, 2005. doi: 10.1524/stnd.2005.23.4.249. URL <https://doi.org/10.1524/stnd.2005.23.4.249>.
- Masashi Sugiyama, Matthias Krauledat, and Klaus-Robert Müller. Covariate shift adaptation by importance weighted cross validation. *Journal of Machine Learning Research*, 8:985–1005, 05 2007a.
- Masashi Sugiyama, Shinichi Nakajima, Hisashi Kashima, Paul Buenau, and Motoaki Kawanabe. Direct importance estimation with model selection and its application to covariate shift adaptation. In J. Platt, D. Koller, Y. Singer, and S. Roweis (eds.), *Advances in Neural Information Processing Systems*, volume 20. Curran Associates, Inc., 2007b. URL [https://proceedings.neurips.cc/paper\\_files/paper/2007/file/be83ab3ecd0db773eb2dc1b0a17836a1-Paper.pdf](https://proceedings.neurips.cc/paper_files/paper/2007/file/be83ab3ecd0db773eb2dc1b0a17836a1-Paper.pdf).

- 
- Baochen Sun and Kate Saenko. Deep coral: Correlation alignment for deep domain adaptation. In Gang Hua and Hervé Jégou (eds.), *Computer Vision – ECCV 2016 Workshops*, pp. 443–450, Cham, 2016. Springer International Publishing. ISBN 978-3-319-49409-8.
- Baochen Sun, Jiashi Feng, and Kate Saenko. *Correlation Alignment for Unsupervised Domain Adaptation*, pp. 153–171. Springer International Publishing, Cham, 2017. ISBN 978-3-319-58347-1. doi: 10.1007/978-3-319-58347-1\_8. URL [https://doi.org/10.1007/978-3-319-58347-1\\_8](https://doi.org/10.1007/978-3-319-58347-1_8).
- Michael Tangermann, Klaus-Robert Müller, Ad Aertsen, Niels Birbaumer, Christoph Braun, Clemens Brunner, Robert Leeb, Carsten Mehring, Kai Miller, Gernot Mueller-Putz, Guido Nolte, Gert Pfurtscheller, Hubert Preissl, Gerwin Schalk, Alois Schlögl, Carmen Vidaurre, Stephan Waldert, and Benjamin Blankertz. Review of the BCI Competition IV. *Frontiers in Neuroscience*, 6, 2012. ISSN 1662-453X. URL <https://www.frontiersin.org/articles/10.3389/fnins.2012.00055>.
- Hemanth Venkateswara, Jose Eusebio, Shayok Chakraborty, and Sethuraman Panchanathan. Deep hashing network for unsupervised domain adaptation. In *Proceedings of the IEEE Conference on Computer Vision and Pattern Recognition (CVPR)*, July 2017.
- Jindong Wang. Everything about transfer learning and domain adaptation, 2018. URL <http://transferlearning.xyz>.
- Shitao Xiao, Zheng Liu, Peitian Zhang, and Niklas Muennighoff. C-pack: Packaged resources to advance general chinese embedding, 2023a.
- Zhiqing Xiao, Haobo Wang, Ying Jin, Lei Feng, Gang Chen, Fei Huang, and Junbo Zhao. Spa: A graph spectral alignment perspective for domain adaptation, 2023b. URL <https://arxiv.org/abs/2310.17594>.
- Andy B Yoo, Morris A Jette, and Mark Grondona. Slurm: Simple linux utility for resource management. In *Workshop on job scheduling strategies for parallel processing*, pp. 44–60. Springer, 2003.
- Kaichao You, Ximei Wang, Mingsheng Long, and Michael Jordan. Towards accurate model selection in deep unsupervised domain adaptation. In Kamalika Chaudhuri and Ruslan Salakhutdinov (eds.), *Proceedings of the 36th International Conference on Machine Learning*, volume 97 of *Proceedings of Machine Learning Research*, pp. 7124–7133. PMLR, 09–15 Jun 2019. URL <https://proceedings.mlr.press/v97/you19a.html>.
- Kun Zhang, Bernhard Schölkopf, Krikamol Muandet, and Zhikun Wang. Domain adaptation under target and conditional shift. In Sanjoy Dasgupta and David McAllester (eds.), *Proceedings of the 30th International Conference on Machine Learning*, volume 28 of *Proceedings of Machine Learning Research*, pp. 819–827, Atlanta, Georgia, USA, 17–19 Jun 2013. PMLR. URL <https://proceedings.mlr.press/v28/zhang13d.html>.
- Yuchen Zhang, Tianle Liu, Mingsheng Long, and Michael I. Jordan. Bridging theory and algorithm for domain adaptation, 2019. URL <https://arxiv.org/abs/1904.05801>.
- Erheng Zhong, Wei Fan, Qiang Yang, Olivier Verscheure, and Jiangtao Ren. Cross validation framework to choose amongst models and datasets for transfer learning. In José Luis Balcázar, Francesco Bonchi, Aristides Gionis, and Michèle Sebag (eds.), *Machine Learning and Knowledge Discovery in Databases*, pp. 547–562, Berlin, Heidelberg, 2010. Springer Berlin Heidelberg. ISBN 978-3-642-15939-8.

---

## A Appendix

# Appendix

**Reproducibility.** The entire code and results of *SKADA-Bench* will be open-sourced and available online. The implementation of the DA methods and scorers is provided along with access to the simulated and real-world datasets. All the performance tables and figures can be reproduced effortlessly, and guidelines with minimal working examples are given to add new DA methods and datasets.

**Roadmap.** In this appendix, we provide additional information regarding the validation procedure used in the literature for each DA method implemented in *SKADA-Bench* in Section B. We provide a detailed description of the data and preprocessing used in *SKADA-Bench* in Section C. In Section D, we give minimal working Python examples to add a new DA method and dataset in *SKADA-Bench*. Finally, we provide the detailed benchmark results in Section E. In particular, the results per dataset can be found in Section E.1. We discuss in Section E.2 the impact of the choice of base estimator on the performance of DA methods for the simulated datasets. The results of each DA method with the supervised scorer on all the datasets are given in Table 20 of Section E.3, which parallels Table 2. A thorough analysis of the effect of using realistic unsupervised scorers is also provided in Section E.6. Finally, the computational efficiency of each DA method is studied in Section E.7 and the hyperparameters used for grid search are given in Section E.8. We display the corresponding table of contents below.

## Table of Contents

<b>B Model selection in Domain Adaptation</b>	<b>19</b>
<b>C Datasets description and preprocessing</b>	<b>20</b>
<b>D Adding new methods and datasets to <i>SKADA-Bench</i></b>	<b>20</b>
D.1 Adding a new DA method . . . . .	21
D.2 Adding a new dataset . . . . .	21
<b>E Benchmark detailed results</b>	<b>22</b>
E.1 Results per datasets . . . . .	22
E.2 Impact of the base estimators on the simulated datasets . . . . .	33
E.3 Unrealistic validation with supervised scorer . . . . .	36
E.4 F1-score of benchmark . . . . .	38
E.5 Comparison of the rank of DA scorer . . . . .	38
E.6 Comparisons between supervised and unsupervised scorers . . . . .	39
E.7 Computational efficiency of the DA methods . . . . .	41
E.8 Hyperparameters grid search for the DA methods and neural networks training . . . . .	42

## B Model selection in Domain Adaptation

Table 4: Validation procedure in Domain Adaptation methods. NA stands for *not applicable* and means that there are no hyperparameters. None means that no validation procedure has been conducted or that it is not specified in the original paper.

	Method	Validation Procedure	Comment
Reweighting	Density Reweight (Sugiyama & Müller, 2005)	None	Bandwidth fixed by Silverman method
	Discriminative Reweight (Shimodaira, 2000)	NA	No hyperparameters
	Gaussian Reweight (Shimodaira, 2000)	None	Not specified in (Shimodaira, 2000)
	KLIEP (Sugiyama et al., 2007b)	Integrated CV	Likelihood CV on target (Sugiyama et al., 2007b)
	KMM (Huang et al., 2006)	None	Fixed data-dependent hyperparameters
	NN Reweight (Loog, 2012)	None	Number of neighbors fixed to one
	MMDTarS (Zhang et al., 2013)	CV	Not specified if done on source or target
Mapping	Coral (Sun et al., 2017)	NA	No hyperparameters
	OT mapping (Courty et al., 2017b)	CV target/CircCV	Unclear in the text
	Lin. OT mapping (Flamary et al., 2020)	NA	No hyperparameters
	MMD-LS (Zhang et al., 2013)	CV	Not specified if done on source or target
Subsp.	SA (Fernando et al., 2013)	2-fold CV on source	-
	TCA (Pan et al., 2011)	Validation on target	Target subset used to tune parameters
	TSL (Si et al., 2010)	None	Not specified in (Si et al., 2010)
Other	JDOT (Courty et al., 2017a)	Reverse CV (Zhong et al., 2010)	-
	OT label prop (Solomon et al., 2014)	NA	No hyperparameters
	DASVM (Bruzzone & Marconcini, 2010a)	Circular Validation (Bruzzone & Marconcini, 2010a)	-

In Table 4, we provide additional information on the validation procedures used in the original papers that proposed the different domain adaptation methods implemented in *SKADA-Bench*. The first column is the name of the method, the second column contains the procedure used to select hyperparameters and the last column provides additional details. What is striking is that many methods do not conduct or specify a validation procedure to select the hyperparameters, which limits the performance of the proposed method on a novel dataset. Several others rely on cross-validation using target data. However, since target labels are typically unavailable in practical scenarios, this validation approach is unrealistic. Overall, many methods have been evaluated with unrealistic or not reproducible validation procedures, making the performance of the proposed methods appear over-optimistic. A key contribution of our work is the extensive comparison of realistic, unsupervised scorers for selecting optimal hyperparameters and base estimators in DA methods.

---

## C Datasets description and preprocessing

The simulated dataset proves that DA methods can work well under the proper shift (see Table 2). However, in real-world applications, we do not have prior knowledge of the type of data shift. Hence, finding the appropriate domain-adaptation method between reweighting, mapping, and subspace methods is a challenging task. In this section, we introduce 8 real-world datasets coming from different fields. Table 1 summarizes the 8 classification datasets used in this benchmark with the corresponding data modality, preprocessing, number of source-target pairs (# adapt), number of classes, samples, and feature dimensions.

**Computer Vision.** First, three computer vision datasets are proposed: Office31 (Koniusz et al., 2017), Office Home (Venkateswara et al., 2017), and MNIST/USPS (Liao & Carneiro, 2015). We create embeddings for Office31 using the Decaff preprocessing method (Donahue et al., 2014) and for Office Home using a pre-trained ResNet50 (He et al., 2016). These embeddings, as well as vectorized MNIST/USPS, are dimensionally reduced with a Principal Component Analysis (PCA). These three datasets encompass 3, 4, and 3 domains, respectively and all pairs of adaptations are used as DA problems. MNIST/USPS contain clear and blurry images digits, Office31 differentiates between images captured by various devices, while for OfficeHome, its by image style.

**NLP.** The second task is Natural Language Processing (NLP). Two datasets are studied: 20Newsgroup (Lang, 1995) and Amazon Review (McAuley et al., 2015). The 20Newsgroup dataset contains 20,000 documents categorized into 4 categories: *talk*, *rec*, *comp*, and *sci*. The learning task is to classify documents across categories. First, the documents are embedded using a Large Language Model (LLM) (Reimers & Gurevych, 2019; Xiao et al., 2023a), and then PCA is applied for dimensionality reduction.

For the Amazon Review dataset, the task is to classify comment ratings. This dataset spans four domains (Books, DVDs, Kitchen, Electronics), and the domain shift results from these varying types of objects. Similar to the 20Newsgroup dataset, comments are embedded using the same LLM and then reduced in dimensionality using a PCA.

**Tabular data.** We propose two tabular datasets. The first one is the Mushroom dataset (Dai et al., 2007), where the task is to classify whether a mushroom is poisonous or not. The two domains are separated according to the mushroom’s stalk shape (enlarging vs. tapering). The tabular data are one-hot-encoded to transform categorical data into numerical data. The second dataset is Phishing (Mohammad et al., 2012). The classification problem involves determining whether a webpage is a phishing or a legitimate one. The domains are separated according to the availability of the IP address. Since the data are already numerical, no preprocessing is done on this dataset.

**Biosignals.** The last task is BCI Motor Imagery. The dataset used is BCI Competition IV (Tangemann et al., 2012), often used in the literature (Barachant et al., 2012) and available in MOABB (Aristimunha et al., 2023). The task is to classify four kinds of motor imagery (right hand, left hand, feet, and tongue) from EEG data. In this dataset, nine subjects are available. The domains are separated based on session number. For each subject, session 1 is considered as the source domain and session 2 is considered as the target domain. The data are multivariate signals. To embed the data, we first compute the covariance and then project this covariance on the Tangent Space as proposed in Barachant et al. (2012).

## D Adding new methods and datasets to SKADA-Bench

Using the `benchopt` framework for this benchmark allows users to easily add novel domain adaptation (DA) methods and datasets. To that end, users should adhere to the `benchopt` (Moreau et al., 2022) conventions. We provide below the guidelines with examples in Python to add a new DA method and a new dataset to SKADA-Bench.

---

## D.1 Adding a new DA method

A new DA method can be easily added with the following:

- Create file with a class called `Solver` that inherits from `DASolver` and place it in the `solvers` folder.
- This class should implement a `get_estimator()` function, which returns a class inheriting from `sklearn.BaseEstimator` and accepts `sample_weight` as fit parameter. In the benchmark we used the Domain Adaptation toolbox SKADA (Gnassounou et al., 2024) that provides many DA estimatos with correct interface.

We provide below an example of Python implementation to add a new DA method to SKADA-Bench.

```
# Python snippet code to add a DA method
from benchmark_utils.base_solver import DASolver
from sklearn.base import BaseEstimator

class MyDAEstimator(BaseEstimator):
    def __init__(self, param1=10, param2='auto'):
        self.param1 = param1
        self.param2 = param2

    def fit(self, X, y, sample_weight=None):
        # sample_weight < 0 are source samples
        # sample_weight >= 0 are target samples
        # y contains -1 for masked target samples
        # Your code here : store stuff in self for later predict
        return self

    def predict(self, X):
        # do prediction on target domain here
        return ypred

    def predict_proba(self, X):
        # do probabilistic prediction on target domain here
        return proba

class Solver(DASolver):
    name = "My_DA_method"

    # Param grid to validate
    default_param_grid = {
        'param1': [10, 100],
        'param2': ['auto', 'manual']
    }

    def get_estimator(self):
        return MyDAEstimator()
```

## D.2 Adding a new dataset

A new DA dataset can be easily added with the following:

- Create a file with a class called `Dataset` that inherits from `BaseDataset` and place it in the `datasets` folder.

- This class should implement a `get_data()` function, which returns a dictionary with keys `X`, `y`, and `sample_domain`.

We provide below an example of Python implementation to add a new dataset to SKADA-Bench.

```
# Python snippet code to add a dataset

from benchopt import BaseDataset
from sklearn.datasets import make_blobs
import numpy as np

class Dataset(BaseDataset):
    name = "example_dataset"

    def get_data(self):
        X_source, y_source = make_blobs(
            n_samples=100, centers=3,
            n_features=2, random_state=0
        )

        X_target, y_target = make_blobs(
            n_samples=100, centers=5,
            n_features=2, random_state=42
        )
        # sample_domain>0 for source samples
        # sample_domain<0 for target samples
        sample_domain = np.array([1]*len(X_source) + [-2]*len(X_target))

        return dict(
            X=np.concatenate((X_source, X_target), axis=0)
            y=np.concatenate((y_source, y_target))
            sample_domain=sample_domain
        )
```

By following these guidelines, users can seamlessly integrate their own datasets and DA methods into SKADA-Bench. It results in a user-friendly benchmark that enables fast, reproducible, and reliable comparisons of common and novel DA methods and datasets. We will provide users with precomputed result files and utilities, allowing them to run only the new methods or datasets. This will speed up new comparisons and avoid unnecessary computations.

## E Benchmark detailed results

### E.1 Results per datasets

In Table 2 of the main paper, the reported performance for each method on a given dataset is an average over the number of shifts, i.e., the number of source-target pairs denoted by `#adapt` in Table 1. In this section, we provide additional details on the performance of methods for each shift in each dataset. These results are presented in separate tables for each dataset

These detailed tables where cell in green denote a gain wrt Train Src (average outside of standard deviation of Train Src) better illustrate the challenges of domain adaptation (DA) methods. They show that not all shifts are equivalent within a given dataset. For example, Table 12 reveals that only 3 shifts in the AmazonReview dataset present a DA problem (defined as a  $> 3\%$  difference in accuracy between Train Src and Train Tgt). While for the other shifts, we achieve similar performance whether we train on source

or target data. Additionally, some specific shifts present a DA problem that no method can successfully address. This can be seen in the `dsl`  $\rightarrow$  `amz` shift in the Office31 dataset, as shown in Table 7. Finally, some DA methods perform consistently across all shifts within a dataset, as demonstrated by the results for the 20Newsgroup dataset in Table 11.

Table 5: Accuracy score for MNIST/USPS dataset for each shift compared for all the methods. A white color means the method does not increase the performance compared to Train Src (Train on the source). Green indicates that the performance improved with the DA methods. The darker the color, the more significant the change.

		MNIST $\rightarrow$ USPS	USPS $\rightarrow$ MNIST	Mean	Rank
	Train Src	0.66 $\pm$ 0.02	0.43 $\pm$ 0.02	0.54 $\pm$ 0.02	12.00
	Train Tgt	0.96 $\pm$ 0.0	0.96 $\pm$ 0.01	0.96 $\pm$ 0.01	1.00
Reweighting	Dens. RW	0.66 $\pm$ 0.02	0.42 $\pm$ 0.02	0.54 $\pm$ 0.02	13.25
	Disc. RW	0.6 $\pm$ 0.02	0.4 $\pm$ 0.02	0.5 $\pm$ 0.02	19.00
	Gauss. RW	0.11 $\pm$ 0.01	0.11 $\pm$ 0.01	0.11 $\pm$ 0.01	20.00
	KLIEP	0.66 $\pm$ 0.02	0.43 $\pm$ 0.02	0.54 $\pm$ 0.02	13.25
	KMM	0.64 $\pm$ 0.02	0.41 $\pm$ 0.03	0.52 $\pm$ 0.02	18.00
	NN RW	0.66 $\pm$ 0.02	0.42 $\pm$ 0.02	0.54 $\pm$ 0.02	12.00
	MMDTarS	0.66 $\pm$ 0.02	0.42 $\pm$ 0.02	0.54 $\pm$ 0.02	12.75
Mapping	CORAL	0.74 $\pm$ 0.01	0.51 $\pm$ 0.01	0.62 $\pm$ 0.01	5.50
	MapOT	0.69 $\pm$ 0.02	0.54 $\pm$ 0.02	0.61 $\pm$ 0.02	4.00
	EntOT	0.66 $\pm$ 0.02	0.54 $\pm$ 0.02	0.6 $\pm$ 0.02	5.00
	ClassRegOT	0.66 $\pm$ 0.01	0.53 $\pm$ 0.06	0.59 $\pm$ 0.04	11.50
	LinOT	0.74 $\pm$ 0.02	0.53 $\pm$ 0.02	0.64 $\pm$ 0.02	3.25
	MMD-LS	0.66 $\pm$ 0.02	0.47 $\pm$ 0.02	0.56 $\pm$ 0.02	8.25
Subspace	JPCA	0.66 $\pm$ 0.02	0.43 $\pm$ 0.02	0.54 $\pm$ 0.02	12.00
	SA	0.71 $\pm$ 0.03	0.36 $\pm$ 0.11	0.54 $\pm$ 0.07	12.00
	TCA	0.08 $\pm$ 0.07	0.11 $\pm$ 0.02	0.09 $\pm$ 0.05	21.00
	TSL	0.66 $\pm$ 0.02	0.43 $\pm$ 0.02	0.54 $\pm$ 0.02	10.50
Other	JDOT	0.73 $\pm$ 0.02	0.53 $\pm$ 0.02	0.63 $\pm$ 0.02	3.50
	OTLabelProp	0.71 $\pm$ 0.03	0.53 $\pm$ 0.02	0.62 $\pm$ 0.02	6.50

Table 6: Accuracy score for MNIST/USPS dataset for each shift compared for all the Deep DA methods. A white color means the method does not increase the performance compared to Train Src (Train on the source). Green indicates that the performance improved with the DA methods. The darker the color, the more significant the change.

	MNIST $\rightarrow$ USPS	USPS $\rightarrow$ MNIST	Mean	Rank
Train Src	0.94	0.76	0.85	5.0
Train Tgt	0.99	0.99	0.99	1.0
DANN	0.94	0.88	0.91	4.0
DeepCORAL	0.97	0.89	0.93	2.5
DeepJDOT	0.96	0.9	0.93	2.5

Table 7: Accuracy score for Office31 dataset for each shift compared for all the methods. A white color means the method does not increase the performance compared to Train Src (Train on the source). Green indicates that the performance improved with the DA methods. The darker the color, the more significant the change.

	anz $\rightarrow$ dsl	anz $\rightarrow$ web	dsl $\rightarrow$ anz	dsl $\rightarrow$ web	web $\rightarrow$ anz	Mean	Rank
Train Src	0.55 $\pm$ 0.04	0.51 $\pm$ 0.03	0.5 $\pm$ 0.02	0.9 $\pm$ 0.02	0.49 $\pm$ 0.01	0.59 $\pm$ 0.02	8.40
Train Tgt	0.94 $\pm$ 0.03	0.95 $\pm$ 0.01	0.78 $\pm$ 0.02	0.95 $\pm$ 0.02	0.77 $\pm$ 0.01	0.88 $\pm$ 0.02	1.00
Reweighting	Dens. RW	0.49 $\pm$ 0.05	0.51 $\pm$ 0.04	0.5 $\pm$ 0.02	0.85 $\pm$ 0.09	0.49 $\pm$ 0.01	0.57 $\pm$ 0.04
	Disc. RW	0.56 $\pm$ 0.06	0.49 $\pm$ 0.03	0.49 $\pm$ 0.02	0.89 $\pm$ 0.03	0.46 $\pm$ 0.01	0.58 $\pm$ 0.03
	Gauss. RW	0.34 $\pm$ 0.03	0.11 $\pm$ 0.04	0.05 $\pm$ 0.02	0.38 $\pm$ 0.04	0.11 $\pm$ 0.03	0.2 $\pm$ 0.03
	KLIEP	0.55 $\pm$ 0.05	0.5 $\pm$ 0.04	0.49 $\pm$ 0.02	0.91 $\pm$ 0.02	0.48 $\pm$ 0.01	0.59 $\pm$ 0.03
	KMM	0.56 $\pm$ 0.06	0.54 $\pm$ 0.04	0.49 $\pm$ 0.03	0.87 $\pm$ 0.03	0.47 $\pm$ 0.02	0.59 $\pm$ 0.03
	NN RW	0.54 $\pm$ 0.04	0.5 $\pm$ 0.03	0.49 $\pm$ 0.02	0.91 $\pm$ 0.01	0.48 $\pm$ 0.01	0.58 $\pm$ 0.02
MMDTarS	0.53 $\pm$ 0.04	0.52 $\pm$ 0.04	0.5 $\pm$ 0.03	0.81 $\pm$ 0.14	0.49 $\pm$ 0.01	0.57 $\pm$ 0.05	10.00
Mapping	CORAL	0.53 $\pm$ 0.04	0.53 $\pm$ 0.03	0.5 $\pm$ 0.03	0.91 $\pm$ 0.03	0.5 $\pm$ 0.01	0.6 $\pm$ 0.03
	MapOT	0.47 $\pm$ 0.03	0.5 $\pm$ 0.04	0.47 $\pm$ 0.01	0.85 $\pm$ 0.03	0.43 $\pm$ 0.01	0.54 $\pm$ 0.03
	EntOT	0.52 $\pm$ 0.03	0.56 $\pm$ 0.02	0.5 $\pm$ 0.03	0.88 $\pm$ 0.02	0.46 $\pm$ 0.01	0.58 $\pm$ 0.02
	ClassRegOT	0.58 $\pm$ 0.07	0.59 $\pm$ 0.04	0.51 $\pm$ 0.02	0.84 $\pm$ 0.04	0.25 $\pm$ 0.25	0.55 $\pm$ 0.08
	LinOT	0.54 $\pm$ 0.05	0.56 $\pm$ 0.05	0.49 $\pm$ 0.02	0.9 $\pm$ 0.02	0.49 $\pm$ 0.01	0.6 $\pm$ 0.03
	MMD-LS	0.55 $\pm$ 0.04	0.51 $\pm$ 0.04	0.49 $\pm$ 0.03	0.9 $\pm$ 0.02	0.48 $\pm$ 0.01	0.59 $\pm$ 0.03
Subspace	JPCA	0.53 $\pm$ 0.04	0.51 $\pm$ 0.02	0.49 $\pm$ 0.02	0.89 $\pm$ 0.01	0.48 $\pm$ 0.01	0.58 $\pm$ 0.02
	SA	0.42 $\pm$ 0.17	0.5 $\pm$ 0.03	0.5 $\pm$ 0.02	0.84 $\pm$ 0.09	0.49 $\pm$ 0.02	0.55 $\pm$ 0.07
	TCA	0.03 $\pm$ 0.01	0.03 $\pm$ 0.0	0.04 $\pm$ 0.0	0.04 $\pm$ 0.0	0.04 $\pm$ 0.0	0.03 $\pm$ 0.0
	TSL	0.55 $\pm$ 0.04	0.51 $\pm$ 0.04	0.49 $\pm$ 0.03	0.9 $\pm$ 0.02	0.49 $\pm$ 0.01	0.59 $\pm$ 0.03
Other	JDOT	0.64 $\pm$ 0.05	0.63 $\pm$ 0.02	0.5 $\pm$ 0.02	0.77 $\pm$ 0.04	0.49 $\pm$ 0.01	0.61 $\pm$ 0.03
	OTLabelProp	0.58 $\pm$ 0.03	0.63 $\pm$ 0.02	0.49 $\pm$ 0.04	0.89 $\pm$ 0.02	NA	0.65 $\pm$ 0.03
							8.75

Table 8: Accuracy score for Office31 dataset for each shift compared for all the deep DA methods. A white color means the method does not increase the performance compared to Train Src (Train on the source). Green indicates that the performance improved with the DA methods. The darker the color, the more significant the change.

	amz→dsl	amz→web	dsl→amz	dsl→web	web→amz	web→dsl	Mean	Rank
Train Src	0.72	0.75	0.61	0.94	0.63	0.99	0.77	4.17
Train Tgt	0.99	1.0	0.87	0.99	0.88	0.99	0.95	1.25
DANN	0.75	0.8	0.64	0.96	0.62	0.98	0.79	3.75
DeepCORAL	0.77	0.77	0.61	0.98	0.63	0.99	0.79	3.33
DeepJDOT	0.79	0.8	0.68	0.97	0.69	1.0	0.82	2.17

Table 9: Accuracy score for OfficeHome dataset for each shift compared for all the methods. A white color means the method does not increase the performance compared to Train Src (Train on the source). Green indicates that the performance improved with the DA methods. The darker the color, the more significant the change.

	art→clipart	art→product	art→realworld	clipart→art	clipart→product	clipart→realworld	product→art	product→clipart	product→realworld	realworld→art	realworld→clipart	realworld→product	Mean	Rank
Train Src	0.34 ± 0.02	0.63 ± 0.01	0.7 ± 0.01	0.46 ± 0.02	0.6 ± 0.01	0.63 ± 0.01	0.5 ± 0.02	0.36 ± 0.02	0.71 ± 0.01	0.63 ± 0.01	0.38 ± 0.01	0.74 ± 0.02	0.56 ± 0.01	10.42
Train Tgt	0.71 ± 0.02	0.92 ± 0.01	0.84 ± 0.01	0.73 ± 0.03	0.91 ± 0.01	0.83 ± 0.01	0.72 ± 0.01	0.7 ± 0.01	0.83 ± 0.01	0.75 ± 0.02	0.7 ± 0.01	0.91 ± 0.01	0.8 ± 0.01	1.00
Dens. RW	0.34 ± 0.02	0.63 ± 0.01	0.71 ± 0.01	0.47 ± 0.02	0.58 ± 0.06	0.63 ± 0.01	0.5 ± 0.02	0.36 ± 0.02	0.71 ± 0.01	0.64 ± 0.01	0.37 ± 0.01	0.73 ± 0.05	0.55 ± 0.02	9.71
Disc. RW	0.32 ± 0.01	0.56 ± 0.03	0.71 ± 0.02	0.42 ± 0.02	0.52 ± 0.01	0.57 ± 0.02	0.53 ± 0.01	0.35 ± 0.02	0.72 ± 0.01	0.63 ± 0.01	0.37 ± 0.01	0.73 ± 0.01	0.54 ± 0.02	13.00
Gauss. RW	0.22 ± 0.01	0.43 ± 0.01	0.59 ± 0.02	0.35 ± 0.01	0.46 ± 0.03	0.48 ± 0.02	0.41 ± 0.02	0.25 ± 0.02	0.61 ± 0.01	0.53 ± 0.01	0.26 ± 0.02	0.67 ± 0.02	0.44 ± 0.02	18.08
KLIEP	0.34 ± 0.02	0.63 ± 0.01	0.7 ± 0.01	0.46 ± 0.02	0.6 ± 0.01	0.63 ± 0.01	0.5 ± 0.02	0.36 ± 0.02	0.71 ± 0.01	0.64 ± 0.01	0.38 ± 0.01	0.74 ± 0.03	0.56 ± 0.02	9.00
RMM	0.32 ± 0.02	0.62 ± 0.01	0.7 ± 0.01	0.45 ± 0.07	0.61 ± 0.02	0.64 ± 0.02	0.48 ± 0.01	0.34 ± 0.02	0.7 ± 0.01	0.58 ± 0.01	0.35 ± 0.04	0.73 ± 0.01	0.54 ± 0.02	13.96
NN RW	0.34 ± 0.02	0.63 ± 0.01	0.7 ± 0.02	0.45 ± 0.02	0.59 ± 0.01	0.61 ± 0.01	0.5 ± 0.02	0.35 ± 0.02	0.71 ± 0.01	0.63 ± 0.01	0.37 ± 0.01	0.74 ± 0.02	0.55 ± 0.02	12.96
MMDTarS	0.34 ± 0.02	0.63 ± 0.01	0.7 ± 0.01	0.46 ± 0.02	0.61 ± 0.01	0.63 ± 0.01	0.5 ± 0.02	0.36 ± 0.02	0.71 ± 0.01	0.64 ± 0.01	0.38 ± 0.01	0.74 ± 0.03	0.56 ± 0.02	7.71
CORAL	0.39 ± 0.02	0.64 ± 0.01	0.7 ± 0.01	0.48 ± 0.02	0.58 ± 0.01	0.61 ± 0.01	0.54 ± 0.02	0.38 ± 0.02	0.72 ± 0.01	0.64 ± 0.01	0.43 ± 0.01	0.75 ± 0.02	0.57 ± 0.01	6.62
MapOT	0.36 ± 0.03	0.53 ± 0.01	0.64 ± 0.01	0.41 ± 0.02	0.52 ± 0.01	0.53 ± 0.01	0.45 ± 0.01	0.37 ± 0.02	0.64 ± 0.01	0.59 ± 0.02	0.41 ± 0.01	0.67 ± 0.02	0.51 ± 0.02	12.42
EntOT	0.38 ± 0.02	0.65 ± 0.01	0.72 ± 0.01	0.5 ± 0.01	0.61 ± 0.02	0.66 ± 0.02	0.55 ± 0.02	0.38 ± 0.01	0.71 ± 0.02	0.65 ± 0.01	0.42 ± 0.01	0.73 ± 0.01	0.58 ± 0.01	5.00
ClassRegOT	0.39 ± 0.02	0.66 ± 0.01	0.73 ± 0.01	0.53 ± 0.01	0.63 ± 0.01	0.67 ± 0.01	0.56 ± 0.03	0.39 ± 0.01	0.72 ± 0.02	0.64 ± 0.01	0.43 ± 0.01	0.74 ± 0.02	0.59 ± 0.01	3.42
LinOT	0.39 ± 0.02	0.64 ± 0.02	0.7 ± 0.01	0.49 ± 0.02	0.59 ± 0.01	0.62 ± 0.01	0.54 ± 0.02	0.38 ± 0.02	0.72 ± 0.01	0.63 ± 0.01	0.43 ± 0.01	0.75 ± 0.03	0.57 ± 0.01	6.54
MMD-LS	0.34 ± 0.02	0.63 ± 0.02	0.7 ± 0.01	0.46 ± 0.02	0.6 ± 0.01	0.62 ± 0.01	0.5 ± 0.02	0.36 ± 0.02	0.71 ± 0.01	0.63 ± 0.02	0.38 ± 0.01	0.74 ± 0.02	0.56 ± 0.01	6.46
JPCA	0.34 ± 0.02	0.63 ± 0.02	0.7 ± 0.01	0.46 ± 0.02	0.6 ± 0.01	0.63 ± 0.01	0.5 ± 0.02	0.35 ± 0.02	0.71 ± 0.01	0.63 ± 0.01	0.38 ± 0.01	0.74 ± 0.02	0.56 ± 0.01	10.58
SA	0.39 ± 0.02	0.64 ± 0.01	0.7 ± 0.01	0.55 ± 0.02	0.5 ± 0.01	0.63 ± 0.01	0.54 ± 0.02	0.38 ± 0.02	0.71 ± 0.02	0.63 ± 0.01	0.41 ± 0.01	0.75 ± 0.03	0.57 ± 0.03	6.58
TCA	0.02 ± 0.01	0.01 ± 0.01	0.02 ± 0.01	0.02 ± 0.01	0.02 ± 0.01	0.02 ± 0.01	0.01 ± 0.01	0.02 ± 0.01	0.02 ± 0.01	0.03 ± 0.01	0.02 ± 0.01	0.02 ± 0.01	0.02 ± 0.01	19.17
JDOT	NA	NA	NA	NA	NA	NA	0.48 ± 0.01	NA	0.65 ± 0.02	NA	NA	NA	NA	16.75
OTLabelProp	0.32 ± 0.02	0.57 ± 0.01	0.66 ± 0.02	0.51 ± 0.02	0.63 ± 0.01	0.63 ± 0.02	0.53 ± 0.01	0.39 ± 0.01	0.7 ± 0.01	0.63 ± 0.02	0.43 ± 0.01	0.74 ± 0.02	0.56 ± 0.01	9.25

Table 10: Accuracy score for OfficeHome dataset for each shift compared for all the deep DA methods. A white color means the method does not increase the performance compared to Train Src (Train on the source). Green indicates that the performance improved with the DA methods. The darker the color, the more significant the change.

	art→clipart	art→product	art→realworld	clipart→art	clipart→product	clipart→realworld	product→art	product→clipart	product→realworld	realworld→art	realworld→clipart	realworld→product	Mean	Rank
Train Src	0.42	0.62	0.75	0.53	0.6	0.62	0.52	0.31	0.73	0.67	0.41	0.76	0.58	4.83
Train Tgt	0.78	0.91	0.86	0.8	0.93	0.85	0.8	0.78	0.86	0.78	0.76	0.92	0.83	1.00
DANN	0.44	0.63	0.73	0.58	0.61	0.62	0.54	0.38	0.75	0.67	0.44	0.76	0.6	4.25
DeepCORAL	0.47	0.64	0.75	0.63	0.59	0.65	0.59	0.39	0.76	0.7	0.45	0.78	0.62	3.00
DeepJDOT	0.47	0.65	0.74	0.63	0.65	0.66	0.59	0.44	0.77	0.71	0.47	0.79	0.63	2.33

Table 11: Accuracy score for 20NewsGroups dataset for each shift compared for all the methods. A white color means the method does not increase the performance compared to Train Src (Train on the source). Green indicates that the performance improved with the DA methods. The darker the color, the more significant the change.

	rec→sci	rec→talk	sci→rec	sci→talk	talk→rec	talk→sci	Mean	Rank
Train Src	0.52 ± 0.03	0.56 ± 0.05	0.54 ± 0.05	0.7 ± 0.01	0.52 ± 0.05	0.71 ± 0.03	0.59 ± 0.04	17.58
Train Tgt	1.0 ± 0.0	1.0 ± 0.0	1.0 ± 0.0	0.99 ± 0.0	1.0 ± 0.0	0.99 ± 0.0	1.0 ± 0.0	1.00
Reweighting	Dens. RW	0.49 ± 0.03	0.56 ± 0.05	0.53 ± 0.05	0.69 ± 0.03	0.52 ± 0.05	0.71 ± 0.03	17.67
	Disc. RW	0.45 ± 0.03	0.61 ± 0.07	0.44 ± 0.02	0.76 ± 0.01	0.57 ± 0.04	0.6 ± 0.03	15.50
	Gauss. RW	0.7 ± 0.07	0.45 ± 0.0	0.66 ± 0.11	0.49 ± 0.01	0.44 ± 0.0	0.48 ± 0.02	17.33
	KLIEP	0.52 ± 0.03	0.56 ± 0.05	0.57 ± 0.1	0.7 ± 0.01	0.52 ± 0.05	0.71 ± 0.03	16.50
	KMM	0.65 ± 0.06	0.71 ± 0.03	0.7 ± 0.06	0.74 ± 0.02	0.65 ± 0.14	0.75 ± 0.03	12.17
	NN RW	0.52 ± 0.06	0.57 ± 0.06	0.54 ± 0.03	0.7 ± 0.01	0.52 ± 0.06	0.71 ± 0.03	16.42
MMDTarS	0.52 ± 0.03	0.57 ± 0.05	0.54 ± 0.05	0.7 ± 0.01	0.52 ± 0.06	0.71 ± 0.03	14.17	
Mappings	CORAL	0.61 ± 0.03	0.79 ± 0.02	0.62 ± 0.01	0.76 ± 0.01	0.78 ± 0.01	0.73 ± 0.02	11.67
	MapOT	0.67 ± 0.02	0.84 ± 0.01	0.68 ± 0.02	0.78 ± 0.02	0.83 ± 0.01	0.76 ± 0.02	7.75
	EntOT	0.82 ± 0.0	0.82 ± 0.02	0.78 ± 0.05	0.87 ± 0.01	0.82 ± 0.02	0.87 ± 0.01	6.50
	ClassRegOT	0.92 ± 0.14	0.93 ± 0.1	0.98 ± 0.01	0.96 ± 0.01	0.99 ± 0.0	0.97 ± 0.0	2.67
	LinOT	0.72 ± 0.02	0.92 ± 0.0	0.72 ± 0.01	0.79 ± 0.11	0.91 ± 0.01	0.83 ± 0.07	6.50
	MMD-LS	0.99 ± 0.0	0.98 ± 0.01	0.99 ± 0.0	0.95 ± 0.01	0.98 ± 0.01	0.96 ± 0.01	3.00
Subspace	JPCA	0.71 ± 0.04	0.72 ± 0.06	0.73 ± 0.05	0.7 ± 0.01	0.84 ± 0.02	0.74 ± 0.04	11.75
	SA	0.83 ± 0.03	0.84 ± 0.01	0.85 ± 0.01	0.87 ± 0.01	0.84 ± 0.03	0.87 ± 0.01	3.83
	TCA	0.59 ± 0.25	0.52 ± 0.08	NA	NA	0.55 ± 0.09	0.56 ± 0.01	15.50
Other	JDOT	0.67 ± 0.02	0.84 ± 0.01	0.68 ± 0.02	0.79 ± 0.02	0.84 ± 0.01	0.77 ± 0.01	8.50
	OTLabelProp	0.78 ± 0.01	0.95 ± 0.01	0.78 ± 0.01	0.84 ± 0.05	0.95 ± 0.01	0.83 ± 0.04	5.00
	DASVM	0.59 ± 0.16	0.77 ± 0.02	0.56 ± 0.11	0.78 ± 0.01	0.84 ± 0.05	0.79 ± 0.02	10.00

Table 12: Accuracy score for AmazonReview dataset for each shift compared for all the methods. A white color means the method does not increase the performance compared to Train Src (Train on the source). Green indicates that the performance improved with the DA methods. The darker the color, the more significant the change.

	Train Src	books→electronics	books→kitchen	books→books	DVD→electronics	DVD→kitchen	electronics→books	electronics→DVD	electronics→kitchen	kitchen→books	kitchen→DVD	kitchen→electronics	Mean	Rank
	0.65 ± 0.03	0.71 ± 0.02	0.77 ± 0.01	0.72 ± 0.01	0.66 ± 0.02	0.72 ± 0.01	0.69 ± 0.01	0.71 ± 0.01	0.75 ± 0.01	0.71 ± 0.02	0.7 ± 0.02	0.71 ± 0.01	0.73 ± 0.01	3.45
	<b>0.71 ± 0.02</b>	<b>0.74 ± 0.01</b>	<b>0.74 ± 0.01</b>	<b>0.74 ± 0.01</b>	<b>0.69 ± 0.03</b>	<b>0.76 ± 0.01</b>	<b>0.72 ± 0.01</b>	<b>0.72 ± 0.01</b>	<b>0.76 ± 0.01</b>	<b>0.72 ± 0.01</b>	<b>0.72 ± 0.01</b>	<b>0.71 ± 0.01</b>	<b>0.73 ± 0.01</b>	1.00
Dens. RW	0.65 ± 0.03	0.71 ± 0.02	0.72 ± 0.01	0.72 ± 0.01	0.65 ± 0.02	0.72 ± 0.01	0.69 ± 0.03	0.71 ± 0.01	0.74 ± 0.01	0.71 ± 0.02	0.7 ± 0.02	0.71 ± 0.01	0.7 ± 0.02	6.82
Disc. RW	0.63 ± 0.01	0.71 ± 0.01	0.72 ± 0.01	0.72 ± 0.01	0.64 ± 0.02	0.7 ± 0.01	0.68 ± 0.01	0.71 ± 0.01	0.73 ± 0.01	0.7 ± 0.02	0.7 ± 0.02	0.7 ± 0.01	0.68 ± 0.02	7.32
Gauss. RW	0.53 ± 0.01	0.62 ± 0.01	0.54 ± 0.06	0.54 ± 0.06	0.38 ± 0.06	0.51 ± 0.15	0.68 ± 0.01	0.62 ± 0.01	0.62 ± 0.01	NA	NA	NA	0.53 ± 0.05	19.33
KLIEP	0.65 ± 0.03	0.69 ± 0.04	0.72 ± 0.01	0.72 ± 0.01	0.66 ± 0.02	0.72 ± 0.01	0.69 ± 0.03	0.75 ± 0.01	0.75 ± 0.01	0.65 ± 0.06	0.68 ± 0.03	0.71 ± 0.01	0.69 ± 0.02	6.30
KMM	0.52 ± 0.04	0.63 ± 0.01	0.6 ± 0.04	0.6 ± 0.04	0.5 ± 0.02	0.64 ± 0.04	0.28 ± 0.2	NA	0.63 ± 0.05	0.66 ± 0.03	0.64 ± 0.03	0.58 ± 0.02	0.57 ± 0.05	16.10
NN RW	0.59 ± 0.05	0.69 ± 0.01	0.71 ± 0.03	0.71 ± 0.03	0.51 ± 0.1	0.66 ± 0.06	0.68 ± 0.03	NA	0.71 ± 0.04	0.7 ± 0.02	0.65 ± 0.02	0.68 ± 0.02	0.66 ± 0.04	10.65
MMDTasS	0.65 ± 0.03	0.7 ± 0.02	0.72 ± 0.01	0.72 ± 0.01	<b>0.67 ± 0.01</b>	0.72 ± 0.01	<b>0.7 ± 0.01</b>	0.71 ± 0.02	0.74 ± 0.01	0.7 ± 0.03	0.7 ± 0.02	0.71 ± 0.02	0.7 ± 0.02	7.55
CORAL	0.62 ± 0.03	<b>0.72 ± 0.01</b>	<b>0.73 ± 0.01</b>	<b>0.73 ± 0.01</b>	0.61 ± 0.01	0.72 ± 0.01	0.69 ± 0.01	0.69 ± 0.01	NA	0.7 ± 0.01	0.7 ± 0.01	0.7 ± 0.02	0.69 ± 0.01	4.56
MapOT	0.6 ± 0.01	0.7 ± 0.0	0.71 ± 0.01	0.71 ± 0.01	0.59 ± 0.01	0.7 ± 0.0	0.68 ± 0.01	0.69 ± 0.01	0.73 ± 0.02	0.69 ± 0.01	0.69 ± 0.01	0.64 ± 0.01	0.67 ± 0.01	9.36
EntOT	0.53 ± 0.01	0.62 ± 0.0	0.64 ± 0.0	0.64 ± 0.0	0.53 ± 0.0	0.62 ± 0.0	0.65 ± 0.0	0.66 ± 0.01	0.74 ± 0.01	0.64 ± 0.0	0.64 ± 0.0	0.54 ± 0.0	0.62 ± 0.0	13.86
ClassRegOT	<b>0.68 ± 0.02</b>	<b>0.72 ± 0.02</b>	0.69 ± 0.03	0.69 ± 0.03	<b>0.67 ± 0.02</b>	0.72 ± 0.02	0.61 ± 0.01	0.61 ± 0.02	0.69 ± 0.03	0.65 ± 0.02	0.65 ± 0.02	0.7 ± 0.02	0.67 ± 0.02	9.00
LinOT	0.64 ± 0.03	<b>0.73 ± 0.01</b>	<b>0.73 ± 0.01</b>	<b>0.73 ± 0.01</b>	0.61 ± 0.01	<b>0.73 ± 0.0</b>	0.69 ± 0.02	0.69 ± 0.02	0.74 ± 0.01	0.71 ± 0.02	0.7 ± 0.02	0.7 ± 0.02	0.7 ± 0.02	3.60
MMD-LS	0.56 ± 0.02	0.54 ± 0.03	0.72 ± 0.01	0.72 ± 0.01	0.63 ± 0.06	0.61 ± 0.16	0.65 ± 0.1	0.55 ± 0.15	NA	0.63 ± 0.11	0.48 ± 0.01	0.71 ± 0.01	0.61 ± 0.07	14.30
JPCA	0.61 ± 0.0	0.69 ± 0.01	0.69 ± 0.01	0.69 ± 0.01	0.63 ± 0.01	0.69 ± 0.0	0.68 ± 0.01	0.68 ± 0.01	0.7 ± 0.01	0.67 ± 0.01	0.68 ± 0.01	0.64 ± 0.01	0.67 ± 0.01	10.14
SA	0.62 ± 0.02	<b>0.72 ± 0.01</b>	<b>0.73 ± 0.02</b>	<b>0.73 ± 0.02</b>	0.62 ± 0.01	0.72 ± 0.01	0.69 ± 0.01	0.69 ± 0.01	0.74 ± 0.02	0.71 ± 0.02	0.7 ± 0.01	0.69 ± 0.03	0.69 ± 0.02	8.27
TCA	0.52 ± 0.0	0.62 ± 0.0	0.64 ± 0.0	0.64 ± 0.0	0.52 ± 0.0	0.62 ± 0.0	0.64 ± 0.0	0.64 ± 0.0	0.62 ± 0.0	0.64 ± 0.0	0.64 ± 0.0	0.52 ± 0.0	0.6 ± 0.0	18.45
TSL	0.65 ± 0.03	0.71 ± 0.02	0.72 ± 0.01	0.72 ± 0.01	0.66 ± 0.02	0.72 ± 0.01	0.64 ± 0.0	0.64 ± 0.0	0.75 ± 0.01	0.71 ± 0.02	0.7 ± 0.02	0.71 ± 0.01	0.7 ± 0.02	5.94
JDOT	0.61 ± 0.01	0.71 ± 0.01	0.72 ± 0.01	0.72 ± 0.01	0.6 ± 0.01	0.7 ± 0.0	0.63 ± 0.01	0.63 ± 0.01	0.71 ± 0.02	0.69 ± 0.02	0.69 ± 0.01	0.67 ± 0.03	0.67 ± 0.01	8.75
OTLabelProp	0.6 ± 0.01	0.69 ± 0.01	0.7 ± 0.01	0.7 ± 0.01	0.59 ± 0.01	0.69 ± 0.01	0.68 ± 0.02	0.69 ± 0.02	0.74 ± 0.01	0.69 ± 0.01	0.69 ± 0.01	0.64 ± 0.01	0.67 ± 0.01	9.32

Table 13: Accuracy score for Mushrooms dataset for each shift compared for all the methods. A white color means the method does not increase the performance compared to Train Src (Train on the source). Green indicates that the performance improved with the DA methods. The darker the color, the more significant the change.

		enl→tap	tap→enl	Mean	Rank
	Train Src	0.67 ± 0.01	0.77 ± 0.01	0.72 ± 0.01	8.50
	Train Tgt	1.0 ± 0.0	1.0 ± 0.0	1.0 ± 0.0	1.00
Reweighting	Dens. RW	0.67 ± 0.01	0.76 ± 0.0	0.71 ± 0.01	9.00
	Disc. RW	0.73 ± 0.06	0.78 ± 0.01	0.75 ± 0.04	4.50
	Gauss. RW	0.56 ± 0.0	0.46 ± 0.0	0.51 ± 0.0	17.50
	KLIEP	0.66 ± 0.02	0.77 ± 0.01	0.72 ± 0.01	10.75
	KMM	0.7 ± 0.02	0.78 ± 0.01	0.74 ± 0.01	6.00
	NN RW	0.67 ± 0.05	0.75 ± 0.01	0.71 ± 0.03	12.00
	MMDTarS	0.7 ± 0.02	0.77 ± 0.01	0.74 ± 0.01	6.00
Mapping	CORAL	0.66 ± 0.02	0.77 ± 0.01	0.72 ± 0.02	11.50
	MapOT	0.65 ± 0.01	0.62 ± 0.02	0.63 ± 0.01	14.00
	EntOT	0.82 ± 0.01	0.67 ± 0.01	0.75 ± 0.01	8.00
	ClassRegOT	0.63 ± 0.01	0.62 ± 0.01	0.62 ± 0.01	15.50
	LinOT	0.72 ± 0.01	0.81 ± 0.01	0.76 ± 0.01	4.00
	MMD-LS	0.85 ± 0.01	NA	0.85 ± 0.01	4.00
	Otspace	JPCA	0.64 ± 0.02	0.78 ± 0.02	0.71 ± 0.02
SA		0.53 ± 0.02	0.86 ± 0.01	0.7 ± 0.02	10.00
Otspace	OTLabelProp	0.68 ± 0.01	0.61 ± 0.01	0.64 ± 0.01	11.50

Table 14: Accuracy score for Phishing dataset for each shift compared for all the methods. A white color means the method does not increase the performance compared to Train Src (Train on the source). Green indicates that the performance improved with the DA methods. The darker the color, the more significant the change.

		$ip\_address \rightarrow no\_ip\_address$	$no\_ip\_address \rightarrow ip\_address$	Mean	Rank
	Train Src	$0.94 \pm 0.01$	$0.88 \pm 0.01$	$0.91 \pm 0.01$	7.0
	Train Tgt	$0.97 \pm 0.01$	$0.97 \pm 0.01$	$0.97 \pm 0.01$	1.0
Reweighting	Dens. RW	$0.94 \pm 0.01$	$0.88 \pm 0.01$	$0.91 \pm 0.01$	6.5
	Disc. RW	$0.94 \pm 0.01$	$0.88 \pm 0.01$	$0.91 \pm 0.01$	9.5
	Gauss. RW	$0.51 \pm 0.0$	$0.41 \pm 0.0$	$0.46 \pm 0.0$	20.0
	KLIEP	$0.94 \pm 0.01$	$0.89 \pm 0.01$	$0.91 \pm 0.01$	5.0
	KMM	$0.94 \pm 0.01$	$0.89 \pm 0.02$	$0.91 \pm 0.01$	6.5
	NN RW	$0.94 \pm 0.01$	$0.89 \pm 0.01$	$0.91 \pm 0.01$	6.5
	MMDTarS	$0.94 \pm 0.01$	$0.88 \pm 0.01$	$0.91 \pm 0.01$	5.5
Mapping	CORAL	$0.93 \pm 0.01$	$0.91 \pm 0.01$	$0.92 \pm 0.01$	5.5
	MapOT	$0.83 \pm 0.01$	$0.84 \pm 0.03$	$0.84 \pm 0.02$	15.0
	EntOT	$0.87 \pm 0.04$	$0.85 \pm 0.03$	$0.86 \pm 0.04$	16.0
	ClassRegOT	$0.87 \pm 0.02$	$0.89 \pm 0.02$	$0.88 \pm 0.02$	9.0
	LinOT	$0.91 \pm 0.01$	$0.9 \pm 0.02$	$0.91 \pm 0.02$	7.0
	MMD-LS	NA	$0.88 \pm 0.01$	$0.88 \pm 0.01$	11.5
Subspace	JPCA	$0.92 \pm 0.01$	$0.89 \pm 0.01$	$0.9 \pm 0.01$	8.0
	SA	$0.9 \pm 0.02$	$0.88 \pm 0.02$	$0.89 \pm 0.02$	11.0
	TSL	$0.88 \pm 0.02$	$0.84 \pm 0.02$	$0.86 \pm 0.02$	14.0
Other	JDOT	$0.8 \pm 0.02$	$0.8 \pm 0.01$	$0.8 \pm 0.02$	18.0
	OTLabelProp	$0.86 \pm 0.01$	$0.86 \pm 0.01$	$0.86 \pm 0.01$	16.0
	DASVM	NA	$0.88 \pm 0.01$	$0.88 \pm 0.01$	15.0

Table 15: Accuracy score for BCI dataset for each shift compared for all the methods. A white color means the method does not increase the performance compared to Train Src (Train on the source). Green indicates that the performance improved with the DA methods. The darker the color, the more significant the change.

	$\lambda$	$\gamma$	$\delta$	$\nu$	$\rho$	$\zeta$	$\xi$	$\eta$	$\theta$	$\iota$	$\kappa$	$\lambda$	$\mu$	$\nu$	$\xi$	$\zeta$	Mean	Rank
Train Src	0.59 ± 0.05	0.51 ± 0.05	0.72 ± 0.05	0.49 ± 0.06	0.39 ± 0.04	0.41 ± 0.06	0.62 ± 0.07	0.69 ± 0.08	0.54 ± 0.1	0.55 ± 0.06	8.56							
Train Tgt	0.74 ± 0.05	0.61 ± 0.07	0.82 ± 0.03	0.52 ± 0.04	0.41 ± 0.08	0.47 ± 0.06	0.75 ± 0.03	0.8 ± 0.03	0.61 ± 0.06	0.64 ± 0.05	1.44							
Dens. RW	0.59 ± 0.06	0.51 ± 0.05	0.72 ± 0.04	0.5 ± 0.06	0.39 ± 0.04	0.4 ± 0.07	0.63 ± 0.06	0.67 ± 0.06	0.53 ± 0.09	0.55 ± 0.06	9.61							
Disc. RW	0.63 ± 0.06	0.51 ± 0.06	0.76 ± 0.05	0.49 ± 0.04	0.4 ± 0.04	0.42 ± 0.08	0.6 ± 0.06	0.68 ± 0.03	0.56 ± 0.09	0.56 ± 0.06	6.89							
Gauss. RW	0.28 ± 0.07	0.25 ± 0.01	0.25 ± 0.01	0.25 ± 0.01	0.25 ± 0.01	0.25 ± 0.01	0.25 ± 0.01	0.25 ± 0.01	0.25 ± 0.01	0.25 ± 0.01	20.44							
KLIEP	0.59 ± 0.05	0.52 ± 0.04	0.71 ± 0.04	0.48 ± 0.07	0.39 ± 0.04	0.41 ± 0.08	0.63 ± 0.07	0.69 ± 0.08	0.55 ± 0.08	0.55 ± 0.06	8.17							
KMM	0.61 ± 0.06	0.45 ± 0.08	0.74 ± 0.05	0.44 ± 0.04	0.31 ± 0.09	0.4 ± 0.07	0.64 ± 0.09	0.64 ± 0.01	0.52 ± 0.07	0.53 ± 0.06	10.89							
NN RW	0.58 ± 0.06	0.45 ± 0.05	0.69 ± 0.03	0.47 ± 0.09	0.36 ± 0.06	0.41 ± 0.05	0.63 ± 0.07	0.68 ± 0.07	0.54 ± 0.08	0.54 ± 0.06	10.67							
MMDTarS	0.59 ± 0.06	0.52 ± 0.04	0.73 ± 0.05	0.5 ± 0.06	0.39 ± 0.04	0.41 ± 0.06	0.62 ± 0.07	0.69 ± 0.07	0.54 ± 0.08	0.55 ± 0.06	8.11							
CORAL	0.77 ± 0.08	0.56 ± 0.06	0.81 ± 0.04	0.49 ± 0.08	0.45 ± 0.05	0.44 ± 0.06	0.73 ± 0.05	0.75 ± 0.1	0.56 ± 0.06	0.62 ± 0.07	2.67							
MapOT	0.61 ± 0.08	0.35 ± 0.04	0.64 ± 0.05	0.39 ± 0.03	0.32 ± 0.04	0.29 ± 0.05	0.53 ± 0.04	0.61 ± 0.08	0.49 ± 0.05	0.47 ± 0.05	11.11							
EntOT	0.67 ± 0.07	0.45 ± 0.05	0.79 ± 0.06	0.37 ± 0.04	0.33 ± 0.06	0.32 ± 0.02	0.67 ± 0.01	0.74 ± 0.07	0.52 ± 0.06	0.54 ± 0.05	9.39							
ClassRegOT	0.61 ± 0.07	0.43 ± 0.07	0.71 ± 0.07	0.4 ± 0.05	0.35 ± 0.04	0.31 ± 0.07	0.62 ± 0.06	0.7 ± 0.05	0.49 ± 0.06	0.51 ± 0.06	12.33							
LinOT	0.76 ± 0.1	0.55 ± 0.05	0.79 ± 0.04	0.48 ± 0.09	0.46 ± 0.06	0.46 ± 0.07	0.71 ± 0.04	0.76 ± 0.09	0.53 ± 0.07	0.61 ± 0.07	3.78							
MMD-LS	0.66 ± 0.1	0.46 ± 0.13	0.63 ± 0.16	0.35 ± 0.11	0.39 ± 0.05	0.34 ± 0.1	0.65 ± 0.08	0.66 ± 0.12	0.49 ± 0.08	0.51 ± 0.1	10.11							
JPCA	0.57 ± 0.07	0.39 ± 0.05	0.72 ± 0.06	0.47 ± 0.07	0.31 ± 0.05	0.33 ± 0.03	0.64 ± 0.06	0.68 ± 0.04	0.49 ± 0.09	0.51 ± 0.06	12.78							
SA	0.74 ± 0.1	0.58 ± 0.09	0.8 ± 0.03	0.48 ± 0.07	0.39 ± 0.04	0.4 ± 0.06	0.66 ± 0.1	0.73 ± 0.07	0.54 ± 0.06	0.59 ± 0.07	6.33							
TCA	0.31 ± 0.09	0.26 ± 0.03	0.24 ± 0.07	0.24 ± 0.1	0.27 ± 0.05	0.26 ± 0.07	0.27 ± 0.06	0.31 ± 0.1	0.29 ± 0.1	0.27 ± 0.07	19.50							
TSL	0.24 ± 0.04	0.26 ± 0.05	0.27 ± 0.05	0.26 ± 0.03	0.23 ± 0.07	0.27 ± 0.04	0.26 ± 0.01	0.24 ± 0.09	0.22 ± 0.03	0.25 ± 0.05	20.00							
JDOT	0.57 ± 0.07	0.37 ± 0.06	0.61 ± 0.05	0.39 ± 0.07	0.28 ± 0.04	0.3 ± 0.03	0.53 ± 0.09	0.62 ± 0.05	0.49 ± 0.05	0.46 ± 0.06	17.00							
OTLabelProp	0.63 ± 0.06	0.4 ± 0.06	0.64 ± 0.05	0.41 ± 0.04	0.35 ± 0.07	0.33 ± 0.06	0.59 ± 0.06	0.66 ± 0.04	0.5 ± 0.09	0.5 ± 0.06	13.11							

Table 16: Accuracy score for BCI dataset for each shift compared for all the deep DA methods. A white color means the method does not increase the performance compared to Train Src (Train on the source). Green indicates that the performance improved with the DA methods. The darker the color, the more significant the change.

	1	2	3	4	5	6	7	8	9	Mean	Rank
Train Src	0.59	0.29	0.67	0.43	0.38	0.29	0.67	0.76	0.67	0.53	2.61
Train Tgt	0.57	0.43	0.71	0.53	0.34	0.29	0.62	0.69	0.79	0.55	2.17
DANN	0.52	0.24	0.55	0.38	0.4	0.22	0.38	0.66	0.64	0.44	4.44
DeepCORAL	0.55	0.26	0.66	0.36	0.48	0.33	0.57	0.72	0.66	0.51	2.72
DeepJDOT	0.53	0.34	0.64	0.43	0.43	0.43	0.57	0.62	0.6	0.51	3.17

## E.2 Impact of the base estimators on the simulated datasets

As mentioned in the main paper, it is possible to partly compensate for the shift by choosing the right base estimator. In this part, we provide the results on the Simulated dataset for three different base estimators: Logistic Regression (LR) in Table 17, SVM in Table 18, and XGBoost in Table 19. Observing the two first rows for covariate shift, we see that with LR (Table 17), there is a significant drop in performance between training on the source v.s. training on the target ( $\sim 10\%$ ), while using SVC (Table 18) only leads to a drop ( $\sim 3\%$ ). Finally, using XGBoost (Table 19) maintains the performance. The reweighting DA methods help compensate for the shift when using a simpler LR estimator. However when using an SVC, as shown in the main paper, the reweighting does not help to compensate for the covariate shift. If we look at the other shifts, the problem is harder. The subspace methods help with subspace shift, and the mapping methods help with the conditional shift.

These Tables show the importance of choosing the right base estimator. It is clear that choosing an appropriate base estimator can partially compensate for some shifts.

Table 17: Accuracy score for simulated datasets compared for all the methods with LR. A white color means the method does not increase the performance compared to Train Src (Train on the source). Green indicates that the performance improved with the DA methods. The darker the color, the more significant the change.

		<i>Cov. shift</i>	<i>Tar. shift</i>	<i>Cond. shift</i>	<i>Sub. shift</i>	Mean	Rank
	Train Src	0.8 ± 0.02	0.81 ± 0.03	0.68 ± 0.03	0.06 ± 0.01	0.59 ± 0.02	10.50
	Train Tgt	0.91 ± 0.02	0.92 ± 0.01	0.79 ± 0.03	0.97 ± 0.01	0.9 ± 0.02	2.00
Reweighting	Dens. RW	0.88 ± 0.03	0.84 ± 0.04	0.66 ± 0.03	0.07 ± 0.02	0.61 ± 0.03	7.50
	Disc. RW	0.55 ± 0.02	0.78 ± 0.05	0.7 ± 0.04	0.06 ± 0.01	0.52 ± 0.03	13.25
	Gauss. RW	0.89 ± 0.02	0.85 ± 0.03	0.64 ± 0.03	0.06 ± 0.01	0.61 ± 0.02	8.00
	KLIEP	0.8 ± 0.02	0.81 ± 0.04	0.69 ± 0.03	0.07 ± 0.02	0.59 ± 0.03	8.25
	KMM	0.84 ± 0.03	0.82 ± 0.05	0.66 ± 0.04	0.07 ± 0.02	0.6 ± 0.04	7.88
	NN RW	0.81 ± 0.02	0.82 ± 0.04	0.67 ± 0.03	0.07 ± 0.01	0.59 ± 0.03	7.75
	MMDTarS	0.8 ± 0.02	0.84 ± 0.04	0.66 ± 0.03	0.07 ± 0.02	0.59 ± 0.03	10.75
Mapping	CORAL	0.73 ± 0.05	0.68 ± 0.11	0.75 ± 0.08	0.04 ± 0.02	0.55 ± 0.06	12.25
	MapOT	0.73 ± 0.03	0.6 ± 0.04	0.79 ± 0.03	0.03 ± 0.01	0.54 ± 0.03	13.75
	EntOT	0.72 ± 0.05	0.61 ± 0.04	0.79 ± 0.03	0.03 ± 0.01	0.54 ± 0.03	12.50
	ClassRegOT	0.87 ± 0.08	0.59 ± 0.04	0.79 ± 0.03	0.03 ± 0.01	0.57 ± 0.04	11.50
	LinOT	0.77 ± 0.03	0.65 ± 0.06	0.76 ± 0.04	0.04 ± 0.02	0.56 ± 0.04	12.00
	MMD-LS	0.7 ± 0.1	0.64 ± 0.06	0.78 ± 0.04	0.38 ± 0.22	0.63 ± 0.1	10.75
Subspace	JPCA	0.8 ± 0.02	0.81 ± 0.03	0.68 ± 0.03	0.06 ± 0.01	0.59 ± 0.02	11.25
	SA	0.8 ± 0.02	0.62 ± 0.04	0.78 ± 0.03	0.04 ± 0.02	0.56 ± 0.03	11.25
	TCA	0.44 ± 0.29	0.49 ± 0.06	0.54 ± 0.11	0.54 ± 0.23	0.5 ± 0.17	15.50
	TSL	0.8 ± 0.02	0.81 ± 0.03	0.68 ± 0.03	0.06 ± 0.01	0.59 ± 0.02	11.00
Other	OTLabelProp	0.73 ± 0.03	0.59 ± 0.04	0.79 ± 0.03	0.03 ± 0.01	0.53 ± 0.03	13.50

Table 18: Accuracy score for simulated datasets compared for all the methods with SVC. A white color means the method does not increase the performance compared to Train Src (Train on the source). Green indicates that the performance improved with the DA methods. The darker the color, the more significant the change.

		<i>Cov. shift</i>	<i>Tar. shift</i>	<i>Cond. shift</i>	<i>Sub. shift</i>	<i>Mean</i>	<i>Rank</i>
	Train Src	0.88 ± 0.03	0.85 ± 0.04	0.66 ± 0.02	0.19 ± 0.03	0.65 ± 0.03	9.38
	Train Tgt	0.92 ± 0.02	0.93 ± 0.02	0.82 ± 0.03	0.98 ± 0.01	0.91 ± 0.02	1.25
Reweighting	Dens. RW	0.88 ± 0.03	0.86 ± 0.04	0.66 ± 0.02	0.18 ± 0.04	0.64 ± 0.03	8.88
	Disc. RW	0.85 ± 0.04	0.83 ± 0.04	0.72 ± 0.04	0.18 ± 0.03	0.64 ± 0.04	10.75
	Gauss. RW	0.89 ± 0.03	0.86 ± 0.04	0.65 ± 0.02	0.21 ± 0.04	0.65 ± 0.03	7.00
	KLIEP	0.88 ± 0.03	0.86 ± 0.04	0.66 ± 0.02	0.19 ± 0.03	0.65 ± 0.03	8.12
	KMM	0.89 ± 0.03	0.87 ± 0.04	0.64 ± 0.04	0.15 ± 0.05	0.64 ± 0.04	9.50
	NN RW	0.89 ± 0.03	0.86 ± 0.04	0.67 ± 0.02	0.15 ± 0.04	0.64 ± 0.03	9.12
	MMDTarS	0.88 ± 0.03	0.86 ± 0.04	0.64 ± 0.03	0.2 ± 0.04	0.65 ± 0.03	9.12
Mapping	CORAL	0.74 ± 0.04	0.7 ± 0.11	0.76 ± 0.08	0.18 ± 0.04	0.59 ± 0.07	11.50
	MapOT	0.72 ± 0.04	0.57 ± 0.04	0.82 ± 0.03	0.02 ± 0.01	0.53 ± 0.03	14.25
	EntOT	0.71 ± 0.04	0.6 ± 0.04	0.82 ± 0.03	0.12 ± 0.06	0.56 ± 0.05	12.75
	ClassRegOT	0.74 ± 0.09	0.58 ± 0.04	0.81 ± 0.03	0.11 ± 0.06	0.56 ± 0.06	12.75
	LinOT	0.73 ± 0.05	0.73 ± 0.08	0.76 ± 0.06	0.18 ± 0.04	0.6 ± 0.06	11.75
	MMD-LS	0.65 ± 0.08	0.68 ± 0.11	0.79 ± 0.05	0.55 ± 0.31	0.67 ± 0.14	10.75
Subspace	JPCA	0.88 ± 0.03	0.85 ± 0.04	0.66 ± 0.02	0.15 ± 0.05	0.64 ± 0.04	11.25
	SA	0.74 ± 0.04	0.68 ± 0.04	0.8 ± 0.03	0.11 ± 0.03	0.58 ± 0.03	12.50
	TCA	0.46 ± 0.21	0.48 ± 0.09	0.55 ± 0.11	0.56 ± 0.2	0.51 ± 0.15	15.62
	TSL	0.88 ± 0.03	0.85 ± 0.04	0.66 ± 0.02	0.19 ± 0.03	0.65 ± 0.03	9.62
Other	OTLabelProp	0.72 ± 0.04	0.58 ± 0.04	0.81 ± 0.04	0.04 ± 0.05	0.54 ± 0.04	14.00

Table 19: Accuracy score for simulated datasets compared for all the methods with XGBoost. A white color means the method does not increase the performance compared to Train Src (Train on the source). Green indicates that the performance improved with the DA methods. The darker the color, the more significant the change.

		<i>Cov. shift</i>	<i>Tar. shift</i>	<i>Cond. shift</i>	<i>Sub. shift</i>	Mean	Rank
	Train Src	0.89 ± 0.02	0.84 ± 0.04	0.66 ± 0.03	0.21 ± 0.03	0.65 ± 0.03	9.25
	Train Tgt	0.89 ± 0.02	0.93 ± 0.02	0.77 ± 0.03	0.98 ± 0.01	0.89 ± 0.02	2.25
Reweighting	Dens. RW	0.88 ± 0.03	0.84 ± 0.03	0.67 ± 0.03	0.22 ± 0.04	0.65 ± 0.03	8.25
	Disc. RW	0.68 ± 0.06	0.84 ± 0.03	0.66 ± 0.03	0.2 ± 0.03	0.6 ± 0.04	12.25
	Gauss. RW	0.87 ± 0.03	0.84 ± 0.03	0.67 ± 0.03	0.22 ± 0.03	0.65 ± 0.03	9.12
	KLIEP	0.88 ± 0.03	0.84 ± 0.03	0.67 ± 0.03	0.21 ± 0.03	0.65 ± 0.03	7.12
	KMM	0.87 ± 0.04	0.84 ± 0.04	0.67 ± 0.04	0.22 ± 0.04	0.65 ± 0.04	7.62
	NN RW	0.88 ± 0.03	0.84 ± 0.04	0.66 ± 0.03	0.2 ± 0.03	0.65 ± 0.03	10.50
	MMDTarS	0.88 ± 0.03	0.86 ± 0.04	0.63 ± 0.03	0.22 ± 0.03	0.65 ± 0.03	7.50
Mapping	CORAL	0.71 ± 0.04	0.71 ± 0.11	0.74 ± 0.08	0.17 ± 0.05	0.58 ± 0.07	12.75
	MapOT	0.7 ± 0.04	0.59 ± 0.03	0.8 ± 0.03	0.17 ± 0.05	0.56 ± 0.04	13.25
	EntOT	0.69 ± 0.05	0.61 ± 0.04	0.8 ± 0.03	0.2 ± 0.02	0.57 ± 0.04	12.25
	ClassRegOT	0.82 ± 0.11	0.59 ± 0.03	0.8 ± 0.03	0.16 ± 0.04	0.59 ± 0.05	12.00
	LinOT	0.72 ± 0.04	0.68 ± 0.06	0.76 ± 0.04	0.19 ± 0.04	0.59 ± 0.05	12.00
	MMD-LS	0.64 ± 0.07	0.68 ± 0.08	0.78 ± 0.04	0.59 ± 0.25	0.67 ± 0.11	10.25
Subspace	JPCA	0.88 ± 0.03	0.84 ± 0.03	0.67 ± 0.03	0.14 ± 0.05	0.63 ± 0.03	10.50
	SA	0.72 ± 0.04	0.69 ± 0.04	0.78 ± 0.03	0.13 ± 0.04	0.58 ± 0.04	11.75
	TCA	0.48 ± 0.05	0.5 ± 0.05	0.51 ± 0.05	0.51 ± 0.06	0.5 ± 0.05	15.50
	TSL	0.89 ± 0.02	0.84 ± 0.04	0.66 ± 0.03	0.21 ± 0.03	0.65 ± 0.03	9.25
Other	OTLabelProp	0.72 ± 0.05	0.59 ± 0.04	0.81 ± 0.04	0.04 ± 0.05	0.54 ± 0.04	13.00

### E.3 Unrealistic validation with supervised scorer

Table 20 shows the results when we choose the supervised scorer that is when validating on target labels. It is important to highlight that this choice is impossible in real life applications due to the lack of target labels. When using the target labels, the method’s parameters are better validated. This can be seen by the significant increase in the table (blue values), which are numerous in this table compared to the one with the selected realistic scorer. For example, the method MMDTarS, which is made for Target shift, compensates all the shift simulated covariate shifts when we select the model with a supervised scorer. When looking at the rank, 11 DA methods have a higher rank than Train Src compared to 9 when using realistic scorer. The findings hold for Deep DA where the accuracy in Table 21 is overall better than when using unsupervised scorers.

Table 20: Accuracy score for all datasets compared for all the methods for simulated and real-life datasets. In this table, each DA method is validated with the supervised scorer. The color indicates the amount of the improvement. A white color means the method is not statistically different from Train Src (Train on source). Blue indicates that the performance improved with the DA methods, while red indicates a decrease. The darker the color, the more significant the change.

		<i>Cov. shift</i>	<i>Tar. shift</i>	<i>Cond. shift</i>	<i>Sub. shift</i>	Office31	OfficeHome	MNIST/USPS	20NewsGroups	AmazonReview	Mushrooms	Phishing	BCI	Rank
	Train Src	0.88	0.85	0.66	0.19	0.65	0.56	0.54	0.59	0.7	0.72	0.91	0.55	10.66
	Train Tgt	0.92	0.93	0.82	0.98	0.89	0.8	0.96	1.0	0.73	1.0	0.97	0.64	1.55
Reweighting	Dens. RW	0.89	0.87	0.67	0.2	0.65	0.56	0.54	0.59	0.7	0.76	0.91	0.55	12.20
	Disc. RW	0.86	0.84	0.73	0.23	0.64	0.54	0.54	0.62	0.69	0.78	0.91	0.56	8.75
	Gauss. RW	0.89	0.86	0.65	0.21	0.22	0.44	0.11	0.54	0.55	0.51	0.46	0.25	16.45
	KLIEP	0.89	0.88	0.66	0.2	0.65	0.56	0.54	0.58	0.7	0.75	0.92	0.55	10.56
	KMM	0.89	0.87	0.67	0.19	0.64	0.55	0.53	0.71	0.66	0.75	0.92	0.54	11.74
	NN RW	0.89	0.86	0.67	0.15	0.65	0.55	0.55	0.59	0.66	0.72	0.91	0.54	9.15
	MMDTarS	0.88	0.93	0.66	0.27	0.65	0.56	0.54	0.59	0.7	0.74	0.91	0.56	10.81
Mapping	CORAL	0.74	0.84	0.82	0.19	0.66	0.57	0.62	0.75	0.7	0.72	0.92	0.62	5.08
	MapOT	0.87	0.63	0.82	0.14	0.6	0.51	0.6	0.77	0.68	0.63	0.84	0.47	10.21
	EntOT	0.89	0.61	0.82	0.47	0.66	0.58	0.63	0.88	0.68	0.81	0.87	0.53	9.40
	ClassRegOT	0.91	0.59	0.82	0.15	NA	0.59	0.66	0.98	0.68	0.89	0.9	0.52	8.25
	LinOT	0.89	0.81	0.81	0.19	0.66	0.58	0.65	0.88	0.71	0.81	0.91	0.61	4.06
	MMD-LS	0.88	0.85	0.81	0.73	0.65	0.56	0.56	0.98	0.69	0.89	NA	0.58	8.22
Subspace	JPCA	0.88	0.85	0.66	0.19	0.65	0.56	0.56	0.84	0.7	0.8	0.9	0.55	8.98
	SA	0.74	0.81	0.8	0.13	0.66	0.57	0.56	0.93	0.7	0.91	0.89	0.59	7.80
	TCA	0.4	0.46	0.5	0.58	0.04	0.02	0.11	0.49	0.61	0.46	0.49	0.27	17.58
	TSL	0.88	0.85	0.66	0.86	0.62	0.48	0.45	0.7	0.69	0.57	0.9	0.26	15.09
Other	JDOT	0.72	0.57	0.82	0.13	0.61	0.41	0.57	0.8	0.67	0.63	0.8	0.46	11.42
	OTLabelProp	0.9	0.76	0.81	0.14	0.66	0.56	0.64	0.89	0.67	0.69	0.86	0.51	10.01
	DASVM	0.89	0.86	0.64	0.12	NA	NA	NA	0.83	NA	0.76	0.86	NA	7.29

Table 21: Accuracy score compared for the Deep methods with the supervised scorer for a selection of real-life datasets.

	MNIST/USPS	Office31	OfficeHome	BCI	Rank
Train Src	0.85	0.77	0.58	0.54	6.19
Train Tgt	0.98	0.96	0.83	0.56	2.07
DeepCORAL	0.93	0.82	0.63	0.54	3.29
DAN	0.91	0.79	0.61	0.55	4.76
DANN	0.9	0.76	0.6	0.42	4.98
DeepJDOT	0.93	0.83	0.63	0.54	2.92
MCC	0.94	0.81	0.66	0.55	2.38
MDD	0.91	0.83	0.58	0.42	4.96
SPA	0.92	0.78	0.56	0.4	5.39

Table 22: F1 score for all datasets compared for all the shallow methods for simulated and real-life datasets. The color indicates the amount of the improvement. A white color means the method is not statistically different from Train Src (Train on source). Blue indicates that the score improved with the DA methods, while red indicates a decrease. The darker the color, the more significant the change.

		<i>Cov. shift</i>	<i>Tar. shift</i>	<i>Cond. shift</i>	<i>Sub. shift</i>	Office31	OfficeHome	MNIST/USPS	20NewsGroups	AmazonReview	Mushrooms	Phishing	BCI	Selected Scorer	Rank
	Train Src	0.88	0.87	0.62	0.17	0.64	0.56	0.52	0.56	0.65	0.72	0.91	0.53		10.95
	Train Tgt	0.92	0.92	0.82	0.98	0.89	0.8	0.96	1.0	0.69	1.0	0.97	0.63		1.70
Reweighting	Dens. RW	0.88	0.88	0.62	0.16	0.61	0.56	0.52	0.55	0.65	0.72	0.91	0.52	IW	12.71
	Disc. RW	0.85	0.86	0.7	0.16	0.63	0.53	0.48	0.56	0.63	0.76	0.91	0.54	CircV	8.39
	Gauss. RW	0.89	0.88	0.61	0.18	0.15	0.4	0.03	0.43	0.49	0.35	0.29	0.1	CircV	16.53
	KLIEP	0.88	0.88	0.62	0.17	0.64	0.55	0.52	0.56	0.65	0.72	0.91	0.52	IW	10.66
	KMM	0.89	0.87	0.6	0.15	0.63	0.54	0.51	0.69	0.5	0.74	0.91	0.49	CircV	11.58
	NN RW	0.89	0.88	0.63	0.14	0.64	0.55	0.52	0.56	0.64	0.71	0.91	0.5	CircV	8.22
	MMDTarS	0.88	0.88	0.6	0.17	0.57	0.56	0.52	0.56	0.65	0.74	0.91	0.53	IW	11.02
Mapping	CORAL	0.74	0.76	0.74	0.16	0.65	0.57	0.62	0.72	0.65	0.72	0.92	0.62	CircV	5.00
	MapOT	0.72	0.65	0.82	0.02	0.59	0.5	0.61	0.76	0.59	0.63	0.84	0.47	PE	10.49
	EntOT	0.71	0.67	0.82	0.12	0.63	0.57	0.59	0.83	0.49	0.75	0.85	0.53	CircV	10.15
	ClassRegOT	0.74	0.66	0.81	0.11	NA	0.53	0.62	0.97	0.67	0.82	0.89	0.52	IW	6.49
	LinOT	0.73	0.78	0.75	0.16	0.65	0.57	0.64	0.81	0.65	0.76	0.91	0.61	CircV	4.20
	MMD-LS	0.77	0.77	0.75	0.54	0.64	0.56	0.54	0.97	0.6	0.85	NA	0.48	MixVal	7.58
Subspace	JPCA	0.88	0.87	0.62	0.14	0.61	0.47	0.5	0.76	0.61	0.78	0.9	0.51	PE	9.55
	SA	0.73	0.74	0.8	0.1	0.64	0.57	0.55	0.88	0.56	0.77	0.89	0.52	CircV	7.95
	TCA	0.51	0.56	0.5	0.61	0.0	0.0	0.02	0.53	0.46	0.44	0.47	0.19	DEV	17.94
	TSL	0.88	0.87	0.63	0.17	0.63	0.47	0.45	0.59	0.58	0.28	0.9	0.21	PE	15.46
Other	JDOT	0.72	0.66	0.82	0.13	0.59	0.41	0.59	0.8	0.61	0.65	0.79	0.46	IW	10.74
	OTLabelProp	0.72	0.67	0.8	0.07	0.65	0.54	0.62	0.86	0.58	0.64	0.86	0.49	CircV	10.80
	DASVM	0.89	0.88	0.61	0.13	NA	NA	NA	0.87	NA	0.82	0.85	NA	MixVal	7.12

#### E.4 F1-score of benchmark

We provide in Table 22 a version of Table 2 where the performance measure reported is the F1-score. It is interesting to note that the dynamic of which methods work best and are the more robust is very similar to the accuracy performance which illustrate the robustness of the benchmark.

#### E.5 Comparison of the rank of DA scorer

To provide a more detailed assessment of the scorers' performance, we present a critical difference diagram of their rankings in Figure 4. The diagram highlights that the unrealistic supervised scorer significantly outperforms all others. Among the unsupervised scorers, CircV and IW achieve the best performance, with their rankings being very close and not statistically different according to a statistical test. Next, we observe a group comprising PE, DEV, and MixVal, where DEV and MixVal are also not statistically distinguishable. Finally, SND emerges as the worst-performing scorer in the benchmark.

To give a more detailed perspective, we present a visualization in Figure 5, showing the rank of each scorer for each DA method. In the right part of the figure, the supervised scorer (in pink) is consistently the top-ranked, as expected, across all methods. Similarly, CircV (in red) and IW (in orange) consistently outperform other scorers.

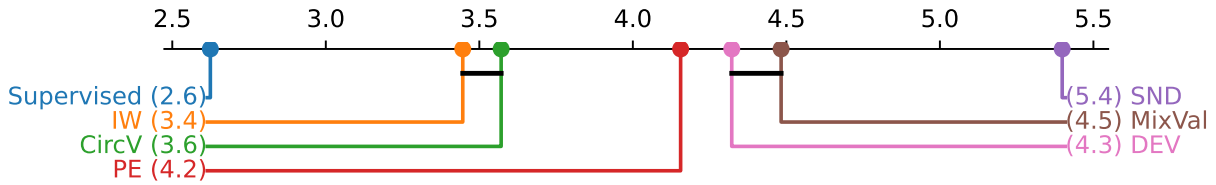


Figure 4: Critical difference diagram of average ranks for scorers, computed across shallow methods and shifts (lower ranks indicate better performance). Black lines between scorers indicate pairs that are not statistically different based on the Wilcoxon test.

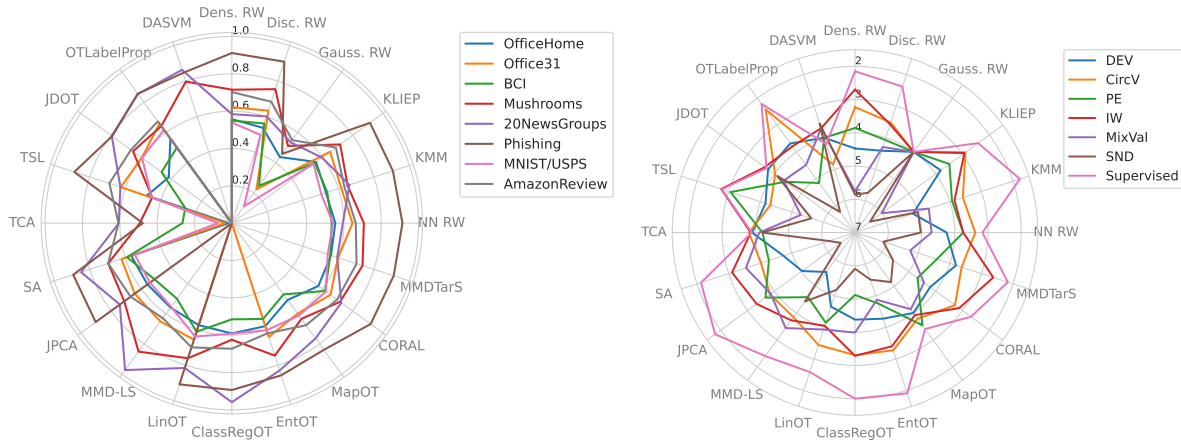


Figure 5: Illustrations as spider plots for all methods of the accuracy on each dataset (left) and the scorers rankings (right). For methods with no accuracy results (NA in Table 2) we replace the value by 0. We provide both spider plot in the same Figure to allow a comparison of the scorer ranking while having the possibility to check the performance for each method.

## E.6 Comparisons between supervised and unsupervised scorers

**Impact on the cross-validation score.** We observe in Figure 6 the cross-validation score as a function of the final accuracy for various DA methods type and for both supervised and unsupervised scorers. As expected, we observe a good correlation between accuracy and cross-validation score with the supervised scorer. An important remark is that the Circular Validation (CircV) (Bruzzone & Marconcini, 2010b) shows some correlation between accuracy and cross-validation score. It indicates that this unsupervised scorer might be the most suitable choice for hyperparameter selection. This is supported by our extended experimental results in Table 2 for which the CircV is selected as the best scorer the most often. A similar trend can be observed for the Importance Weighted (IW) (Sugiyama et al., 2007a) which is also confirmed in Table 2.

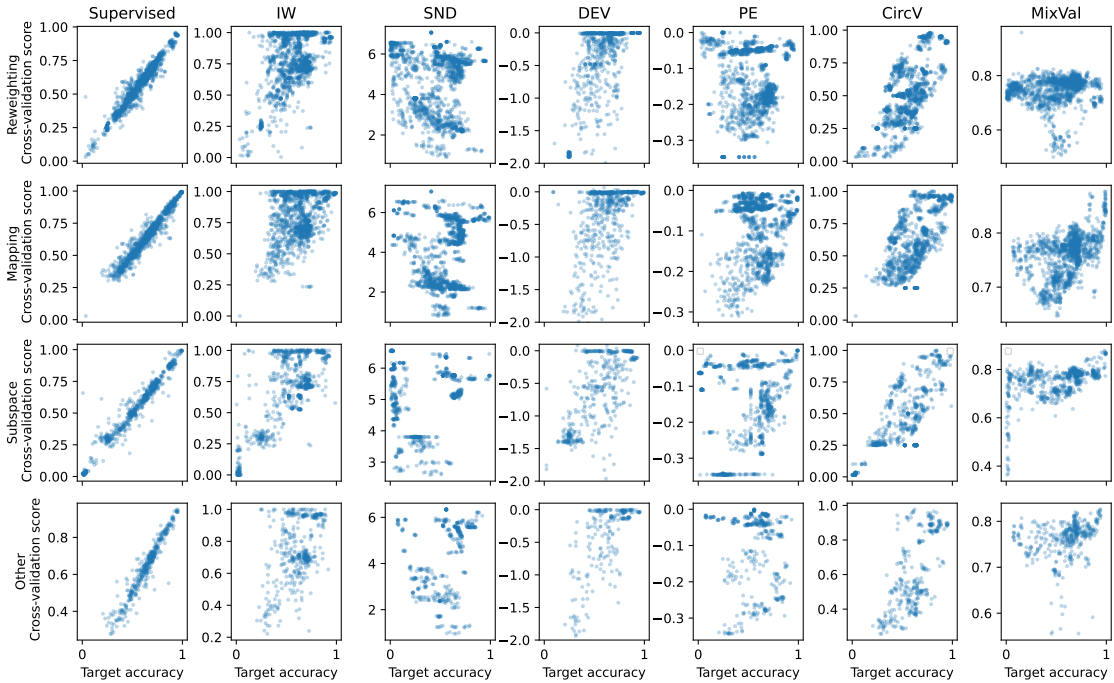


Figure 6: Cross-val score as a function of the accuracy for various DA methods and different supervised and unsupervised scorers. Each point represents an inner split with a DA method (color of the points) and a dataset. A good scorer should have a score that correlates with the target accuracy.

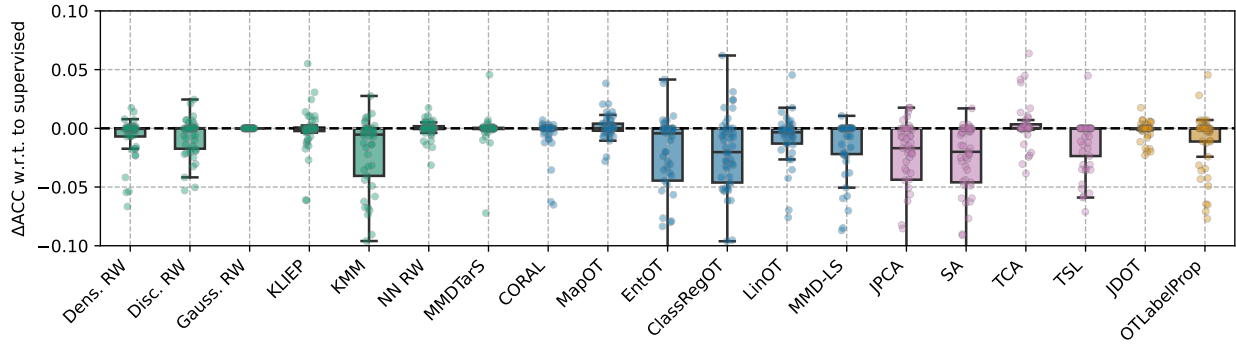


Figure 7: Change of accuracy of the DA methods with the best realistic unsupervised scorer (Table 2) w.r.t. the supervised scorer.

**Supervised scorer v.s. the best realistic unsupervised scorer.** We plot the loss in performance of the DA methods with the best realistic unsupervised scorer compared to using the supervised scorers in Figure 7.

**Supervised scorer v.s. realistic unsupervised scorers.** We present a scatter plot in Figure 8 and Figure 9, the accuracy of different DA methods using both supervised scorer and unsupervised scorer. In this figure, points below the diagonal indicate a decrease in performance when using the unsupervised scorer compared to the supervised one. The colors represent different types of DA methods. We can see that the SND, DEV and PE scorers all lead to a large performance loss compared to the supervised scorer. While IW and CircV results are much more concentrated near the diagonal, indicating a small loss in performance. This concentration explains why these two scorers have been selected as the best scorers for most of the methods in Table 2.

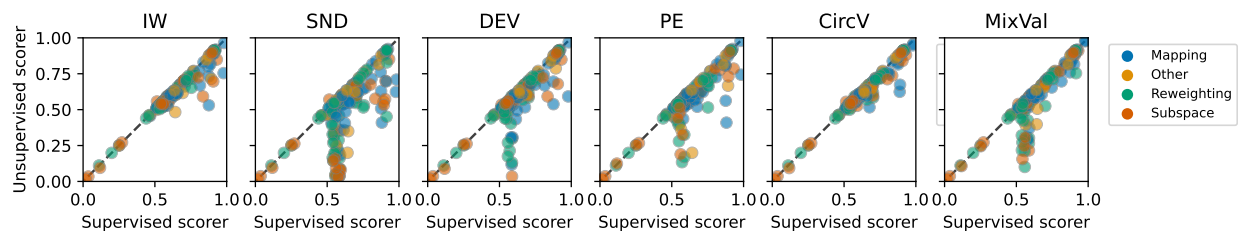


Figure 8: Accuracy of the DA methods using unsupervised scorers as a function of the accuracy with the supervised scorer. Colors represent the type of DA methods.

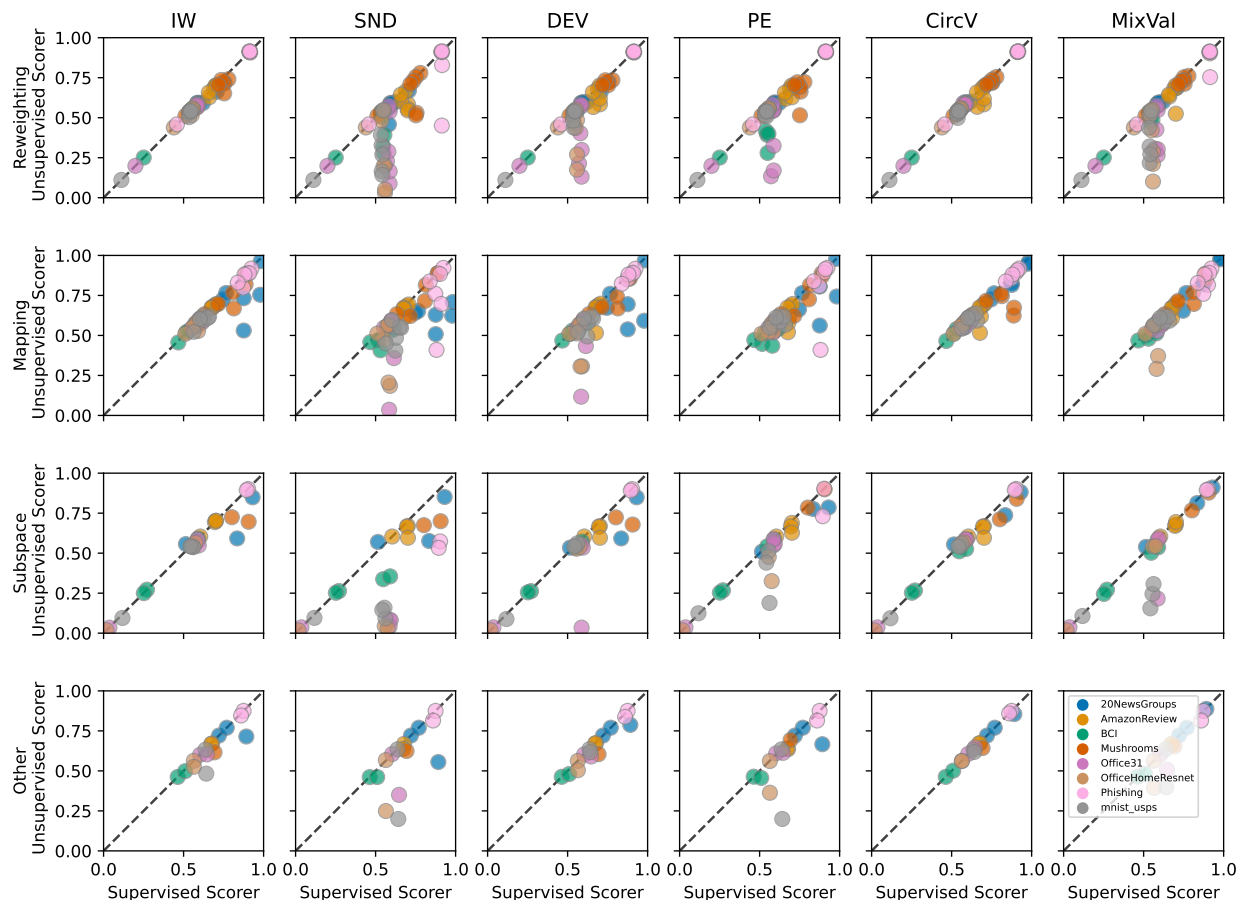


Figure 9: Accuracy of the DA methods using unsupervised scorers as a function of the accuracy with the supervised scorer for the different types of DA methods. Points below the diagonal represent a decrease in performance when using the unsupervised scorer compared to the supervised one. Colors represent the dataset on which the DA method is applied.

## E.7 Computational efficiency of the DA methods

Figure 10 shows the average computation time for training and testing each method. These results are based on one outer split, while we ran the benchmarks for five outer splits. Each method has a different time complexity. Interestingly, more time-consuming methods are not necessarily more performant than others. For instance, the highest-ranked methods—LinOT, CORAL, and SA—also have some of the lowest training

and testing times. It’s also worth noting that during the experiments, we enforced a 4-hour timeout. Thus, the more time-intensive methods might have been even slower without this timeout.

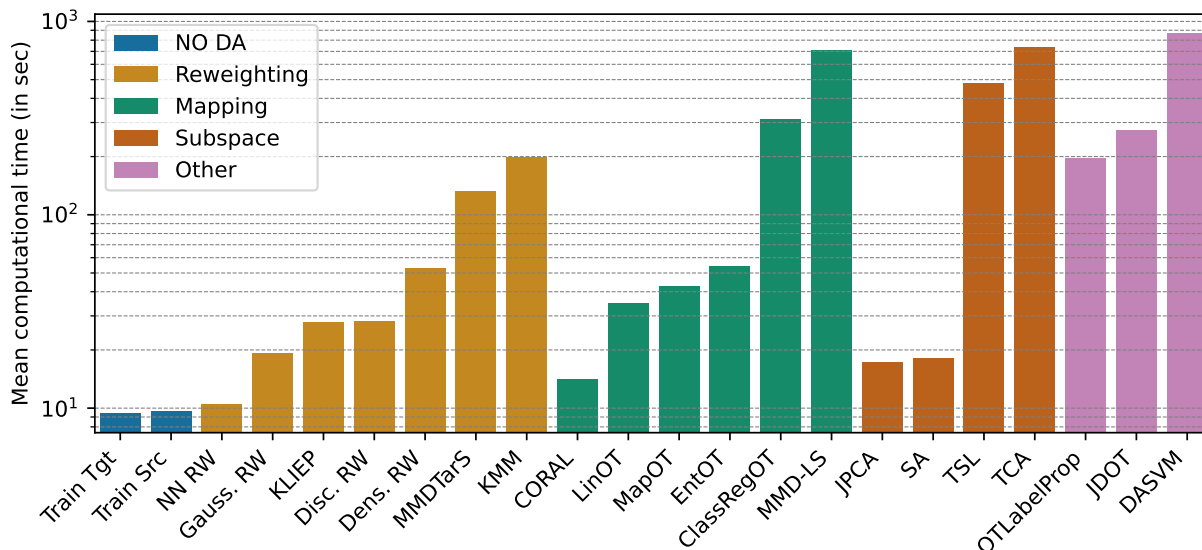


Figure 10: Mean computing time to train and test each method for every experiment outer split.

### E.8 Hyperparameters grid search for the DA methods and neural networks training

In this section, we first report the grids of hyperparameters used in our grid search for each DA method.

We also detail the configuration and hyperparameter grids for training neural networks in our Deep DA benchmark. We provide an overview of the key settings for each dataset, including batch sizes, optimizer parameters, learning rates, and the number of training epochs. Additionally, we outline the hyperparameter grids used for grid search across the Deep DA methods.

Table 23: Hyperparameter grids used in the grid search for each DA method. The hyperparameter grids were designed to be minimal yet expressive, allowing each method to perform optimally. We selected parameters based on what seemed most reasonable, according to our best knowledge.

Method	Hyperparameter Grid
KLIEP	'cv': [5], 'gamma': [0.0001, 0.001, 0.01, 0.1, 1.0, 10.0, 100.0, 1000.0, 'auto', 'scale'], 'max_iter': [1000], 'n_centers': [100], 'random_state': [0], 'tol': [1e-06]
KMM	'B': [1000.0], 'gamma': [0.0001, 0.001, 0.01, 0.1, 1.0, 10.0, 100.0, 1000.0, None], 'max_iter': [1000], 'smooth_weights': [False], 'tol': [1e-06]
NN RW	'laplace_smoothing': [True, False]
MapOT	'max_iter': [1000000], 'metric': ['sqeuclidean', 'cosine', 'cityblock'], 'norm': ['median']
JPCA	'n_components': [1, 2, 5, 10, 20, 50, 100]
SA	'n_components': [1, 2, 5, 10, 20, 50, 100]
TCA	'kernel': ['rbf'], 'mu': [10, 100], 'n_components': [1, 2, 5, 10, 20, 50, 100]
CORAL	'assume_centered': [False, True], 'reg': ['auto']
MMDTarS	'gamma': [0.0001, 0.001, 0.01, 0.1, 1.0, 10.0, 100.0, 1000.0, None], 'max_iter': [1000], 'reg': [1e-06], 'tol': [1e-06]
ClassRegOT	'max_inner_iter': [1000], 'max_iter': [10], 'metric': ['sqeuclidean', 'cosine', 'cityblock'], 'norm': ['lpl1'], 'tol': [1e-06], '(reg_cl, reg_e)': [(0.1, 0.1), (0.5, 0.5), (1.0, 1.0)]
Dens. RW	'bandwidth': [0.01, 0.1, 1.0, 10.0, 100.0, 'scott', 'silverman']
Disc. RW	'domain_classifier': ['LR', 'SVC', 'XGB']
Gauss. RW	'reg': ['auto']
DASVM	'max_iter': [200]
JDOT	'alpha': [0.1, 0.3, 0.5, 0.7, 0.9], 'n_iter_max': [100], 'thr_weights': [1e-07], 'tol': [1e-06]
EntOT	'max_iter': [1000], 'metric': ['sqeuclidean', 'cosine', 'cityblock'], 'norm': ['median'], 'reg_e': [0.1, 0.5, 1.0], 'tol': [1e-06]
LinOT	'bias': [True, False], 'reg': [1e-08, 1e-06, 0.1, 1, 10]
TSL	'base_method': ['fda'], 'length_scale': [2], 'max_iter': [300], 'mu': [0.1, 1, 10], 'n_components': [1, 2, 5, 10, 20, 50, 100], 'reg': [0.0001], 'tol': [0.0001]
MMD-LS	'gamma': [0.01, 0.1, 1, 10, 100], 'max_iter': [20], 'reg_k': [1e-08], 'reg_m': [1e-08], 'tol': [1e-05]
OTLabelProp	'metric': ['sqeuclidean', 'cosine', 'cityblock'], '(n_iter_max, reg)': [(10000), [None]], [(100), [0.1, 1]]

Table 24: Configuration of Deep learning models for each dataset. This includes recommended Batch sizes, optimizer settings, learning rates, and maximum epochs.

Dataset	Configuration
mnist_usps	<ul style="list-style-type: none"> <li>• <b>Neural net:</b> 2-layer CNN</li> <li>• <b>Batch size:</b> 256</li> <li>• <b>Optimizer:</b> SGD, momentum=0.6, weight_decay=1e-5</li> <li>• <b>Learning rate:</b> 0.1</li> <li>• <b>Epochs:</b> 20</li> <li>• <b>Learning rate scheduler:</b> LRScheduler(StepLR, step_size=10, gamma=0.2)</li> </ul>
office31	<ul style="list-style-type: none"> <li>• <b>Neural net:</b> ResNet50</li> <li>• <b>Batch size:</b> 128</li> <li>• <b>Optimizer:</b> SGD, momentum=0.2, weight_decay=1e-5</li> <li>• <b>Learning rate:</b> 0.5</li> <li>• <b>Epochs:</b> 30</li> <li>• <b>Learning rate scheduler:</b> StepLR, step_size=10, gamma=0.2</li> </ul>
officehome	<ul style="list-style-type: none"> <li>• <b>Neural net:</b> ResNet50</li> <li>• <b>Batch size:</b> 128</li> <li>• <b>Optimizer:</b> SGD, momentum=0.6, weight_decay=1e-5</li> <li>• <b>Learning rate:</b> 0.05</li> <li>• <b>Epochs:</b> 20</li> <li>• <b>Learning rate scheduler:</b> StepLR, step_size=10, gamma=0.2</li> </ul>
bci	<ul style="list-style-type: none"> <li>• <b>Neural net:</b> FBCSPNet</li> <li>• <b>Batch size:</b> 64</li> <li>• <b>Optimizer:</b> AdamW</li> <li>• <b>Learning rate:</b> 0.000625</li> <li>• <b>Epochs:</b> 200</li> <li>• <b>Learning rate scheduler:</b> CosineAnnealingLR</li> </ul>

Table 25: Hyperparameter grids used in the grid search for each Deep DA method. The hyperparameter grids were designed to be minimal yet expressive, allowing each method to perform optimally. We selected parameters based on what seemed most reasonable, according to our best knowledge.

Method	Hyperparameter Grid
DANN	'reg': [0.001, 0.01, 0.1, 1.0]
DeepCORAL	'reg': [0.00001, 0.0001, 0.001, 0.01, 0.1, 1.0, 10.0, 100.0, 1000.0]
DeepJDOT	'reg_cl': [0.0001, 0.001, 0.01] 'reg_dist': [0.0001, 0.001, 0.01]
DAN	'reg': [0.00001, 0.0001, 0.001, 0.01, 0.1, 1.0, 10.0, 100.0, 1000.0]
MCC	'reg': [0.01, 0.1, 1] 'temperature': [1, 2, 3]
MDD	'reg': [0.001, 0.01, 0.1] 'gamma': [1, 3]
SPA	'reg': [0.001, 0.01, 0.1, 1] 'reg_nap': [0, 1]